

407471

Wright Aeronautical Serial Report No. CTR.00-275

Final Report

THE EVALUATION OF A LIQUID METAL REGENERATOR
FOR
A 3750 HP TURBOPROP ENGINE

May 15, 1963

Wright Aeronautical Division

Wright Aeronautical Serial Report No. CTR.00-275

Final Report

THE EVALUATION OF A LIQUID METAL REGENERATOR
FOR
A 3750 HP TURBOPROP ENGINE

In Fulfillment of Item 7, Contract NOW62-0601-c

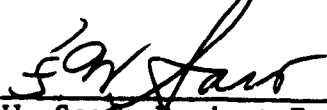
with

Power Plant Division RAPP-14
Bureau of Naval Weapons
Washington 24, D. C.

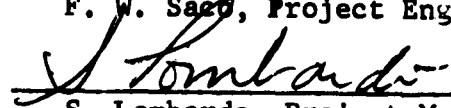
May 15, 1963

Written by:

L. R. Cox J. Horvath
R. Gill F. W. Saco
R. Stevens



F. W. Saco, Project Engineer



S. Lombardo, Project Manager

TABLE OF CONTENTS

<u>Subject</u>	<u>Pages</u>
1. OBJECTIVES	1-1
2. SUMMARY	2-1 through 2-3
3. CONCLUSIONS	3-1
4. RECOMMENDATIONS	4-1
5. DESIGN OF HEAT EXCHANGERS	5-1 through 5-12
5.1.1 Design of Test Heat Exchangers	5-1
5.1.2 Selection of Engine Cycle	5-2
5.1.3 Optimization Studies	5-4
5.1.4 Design of Study Engine	5-5
5.1.5 Take-Off Considerations for Study Engine	5-6
5.2.1 Mechanical Design, Compressor Heat Exchanger	5-7
5.2.2 Mechanical Design, Turbine Heat Exchanger	5-9
5.3 Study Engine, Mechanical Design	5-10
6. FABRICATION OF HEAT EXCHANGERS	6-1 through 6-5
6.1 Heat Transfer Elements	6-1
6.2 Turbine Heat Exchanger	6-3
6.3 Compressor Heat Exchanger	6-4
6.4 Weight of Test Heat Exchanger	6-5
7. TEST EQUIPMENT	7-1 through 7-6
7.1 Description of Test Rig	7-1
7.2 Liquid Metal System	7-2
7.3 Liquid Metal Pump	7-4
7.4 Instrumentation	7-5
7.5 Cold Start Rig	7-6
8. TEST PROGRAM	8-1 through 8-5
8.1 Rig Tests	8-1
8.2 Liquid Metal Thermal Convection Loops	8-3
8.3 Low Temperature Liquid Metal Alloys	8-4

TABLE OF CONTENTS (Cont'd)

<u>Subject</u>	<u>Pages</u>
9. RESULTS AND DISCUSSION	9-1 through 9-7
9.1 General	9-1
9.2 Durability	9-1
9.3 Performance	9-2
9.4 Liquid Metal	9-3
9.5 Fouling	9-4
9.6 Liquid Metal Pump	9-4
9.7 Liquid Metal Alloys	9-5
9.8 Analytical Methods, References	9-6
10. LIST OF SYMBOLS	10-1 through 10-2

FIGURES AND TABLES

(Figures appear in pages adjacent to the page of reference)

<u>Number</u>	<u>Title</u>	<u>Ref. Page</u>
5.1-1	Core Weight Vs. Effectiveness	5-3
5.1-2	Core Weight Vs. Effectiveness Ratio	5-4
5.1-3	Weight-Effectiveness (Downstream Location)	5-5
5.1-4	Weight-Effectiveness (Interstage Location)	5-5
5.1-5	Comparative Regenerator Designs - Study Engine (TABLE)	5-7
5.2-1	Compressor Heat Exchanger, 120° Sector	5-8
5.2-2	Compressor Heat Exchanger, Mock-Up	5-8
5.2-3	Compressor Heat Exchanger, Header Welding	5-8
5.2-4	Bowed Heat Transfer Element	5-9
5.2-5	Turbine Heat Exchanger	5-9
5.2-6	Offset Return Serpentine	5-10
5.2-7	Turbine Heat Exchanger - Tube Support	5-10
5.2-8	Turbine Heat Exchanger - Sub-Assemblies	5-10
5.3-1	Configuration - Regenerated Study Engine	5-10
5.3-2	Liquid Metal Regenerative System	5-11
5.3-3	Regenerator Component Weights, Study Engine (TABLE)	5-12
6.1-1	Heat Transfer Elements	6-1
6.1-2	Cladding Discontinuities	6-1
6.1-3	Finned Tube Cross-Section, Good Braze	6-2
6.1-4	Finned Tube Cross-Section, Poor Braze	6-2

FIGURES AND TABLES (Cont'd)

<u>Number</u>	<u>Title</u>	<u>Ref. Page</u>
6.2-1	Turbine Heat Exchanger - Tube Welding	6-3
6.2-2	Tube-To-Header Joint Designs	6-3
6.2-3	Turbine Heat Exchanger - Half Section	6-3
6.3-1	Micro-photograph - Burned Tube	6-4
7.1-1	Test Rig - Sectional Diagram	7-1
7.1-2	Test Rig - Photograph	7-1
7.2-1	Liquid Metal System - Schematic	7-2
7.3-1	Liquid Metal Pump	7-4
7.3-2	Liquid Metal Pump Test Loop	7-4
7.4-1	Instrumentation List	7-5
7.5-1	Test Apparatus for Cold Start	7-6
8.2-1	Convection Loops - Compatibility Study	8-3
8.2-2	Compatibility Study - Heat Transfer Elements After Test	8-3
8.2-3	Compatibility Study - Head and Tube Sheet After Test	8-3
9.2-1	Summary of Operating Conditions (TABLE)	9-1
9.3-1	System Temperatures Vs. NaK Flow	9-2
9.3-2	Overall Effectiveness Vs. NaK Flow (3.153 lb./sec., Gas)	9-2
9.3-3	Overall Effectiveness Vs. NaK Flow (3.944 lb./sec., Gas)	9-2
9.3-4	Overall Effectiveness Vs. NaK Flow (4.556 lb./sec., Gas)	9-2

FIGURES AND TABLES (Cont'd)

<u>Number</u>	<u>Title</u>	<u>Ref. Page</u>
9.3-5	Pressure Drop Vs. Flow Factor (Turbine Heat Exchanger)	9-3
9.3-6	Pressure Drop Vs. Flow Factor (Compressor Heat Exchanger)	9-3
9.5-1	Turbine Heat Exchanger After 40 Hours Operation	9-4
9.5-2	Compressor Heat Exchanger, Downstream Face	9-4
9.5-3	Compressor Heat Exchanger, Upstream Face	9-4
9.5-4	Performance Vs. Time, Continuous Running	9-4
9.7-1	Cesium-NaK Alloys, Liquid/Solid Ratios (TABLE)	9-5

1. OBJECTIVES

Curtiss-Wright Corporation was awarded a contract by the Department of the Navy, Bureau of Naval Weapons, to conduct an evaluation of a liquid metal regenerator system for a 3750 HP turboprop engine of low fuel consumption. This contract included the design, fabrication, and rig testing of flight weight liquid metal heat exchangers.

This report covers the work performed in fulfillment of the following particular major objectives:

- 1) To design a liquid metal regenerator system for a typical 3750 HP turboprop engine having low fuel consumption.
- 2) To fabricate 120° sectors of full size liquid metal heat exchangers of flight weight design.
- 3) To evaluate the performance of the liquid metal heat exchangers in a regenerator system by rig tests.
- 4) To demonstrate the durability of the heat exchangers and the liquid metal regenerator system by rig tests.

Achievement of these objectives and a complete evaluation of liquid metal regenerator systems required fulfilling the following further objectives relative to the components of the liquid metal regenerator system:

- 5) To extend the state-of-the-art of fabricating high temperature finned tubes in order to obtain advanced heat transfer elements for the test heat exchangers.
- 6) To procure a prototype liquid metal pump to demonstrate principals of operation applicable to the design of flight type pumps for liquid metal regenerator systems.
- 7) To investigate feasibility of new liquid metal alloys particularly suited for flight type liquid metal regenerator systems operating under extremely cold starting conditions.

2. SUMMARY

It is characteristic of current turboprop engines that specific fuel consumption increases significantly as power level is reduced. Since the Navy's advanced AEW and ASW aircraft must cruise for long periods of time at low power settings, the specific fuel consumption at cruise conditions becomes an important parameter in determining endurance range of the aircraft. The use of a regenerative-cycle power plant is recognized as a means of achieving the improved part-load fuel consumption required to meet the performance objectives of the aircraft. Past engine design studies, using conventional heat exchange systems to effect regeneration, have resulted in heavy and cumbersome configurations which discouraged serious consideration of this cycle. This report describes a light-weight compact engine arrangement in which the heat exchange of the regenerative cycle is accomplished by the use of a liquid metal heat transfer system. In addition, this report describes the component test and evaluation program which established the feasibility of the proposed regenerator component.

In the liquid metal regenerator system, heat energy of the turbine discharge is transferred to the liquid metal in the turbine heat exchanger. The heat thus acquired by the liquid metal, which is continuously pumped through the heat exchanger system, is released by the compressor heat exchanger to the compressor discharge air. The liquid metal transport fluid used in this evaluation program was an alloy of sodium and potassium (NaK).

The design evaluation program consisted of studying the mechanical arrangements of a liquid metal regenerative turboprop engine, sized at 3750 HP normal rating and 4150 HP take-off rating. The cycle used in this study was based on typical high-performance components, with the compressor pressure ratio fixed at 12.6 to 1 and the maximum burner temperature fixed at 2200°F. The regenerator component was designed for an effectiveness of 70% at the 35% normal power rating for the 1500 feet altitude, 225 knots cruise condition.

The mechanical design objective in this evaluation was to minimize departures from conventional turboprop engine arrangements, particularly in air and gas flow paths. Emphasis was placed on maintaining an in-line engine arrangement with minimum frontal area. The results of the study showed that with the liquid metal heat exchanger system it was possible to arrive at a compact, in-line turboprop engine arrangement. The maximum diameter of the engine was less than 31 inches, and the total weight of the heat exchanger system added to the engine was 386 pounds for 70% effectiveness and 4% core pressure loss. In terms of specific weight, the regenerator system accounts for only 0.093 pounds per horsepower.

Serpentine finned tube elements were used as the basic heat transfer elements in the design. The liquid metal regenerative system is composed of sectors, in each of which a compressor and turbine heat exchanger is interconnected with a hermetically sealed liquid metal circuit. This concept allows individual segments of the regenerator system to be installed or removed without disconnection of liquid metal lines. This important feature of the design was made possible by the choice of an electro-dynamic pump which required no mechanical connection between the pump and the liquid metal loop.

Full-scale 120° sectors of the regenerator system were fabricated, using the light-weight high performance concepts developed in the study evaluation program. A test program conducted on the regenerator system, which involved over one hundred (100) hours of successful operation under simulated engine conditions, demonstrated the basic mechanical feasibility of the system. However, uneven distribution of the gas to the heat exchangers by the sectorized diffusers of the test rig caused a scattering of the data to the extent that close agreement of heat balances in the system could not be attained.

In addition to these tests, approximately 4,000 hours of independent liquid metal loop testing at simulated engine temperatures was conducted to demonstrate the materials-compatibility with respect to liquid metal.

A limited investigation of NaK characteristics under cold start-up conditions was conducted. Engine start-up without the use of auxiliary heating of the NaK is obviously desirable. Low melting point alloys hold the potential of eliminating the requirement of initial heating. Sodium-potassium alloys can be proportioned to retain some degree of fluidity at temperatures as low as 12°F. Laboratory experiments have shown that the freezing point of NaK alloys can be further depressed (-65°F) by the addition of cesium. In the start-up tests of this investigation, superior cold-start performance under simulated engine conditions with a 10% cesium NaK alloy, at temperatures as low as -15°F, have been demonstrated.

The results of the program can be summarized as follows:

1. Application of a liquid metal regenerator system to a turboprop engine results in a compact, low frontal-area, in-line engine, with minimum disturbances of air and gas flow.
2. Successful operation of the liquid metal regenerator system for over 100 hours at various simulated engine conditions and extreme ranges of operating temperatures has demonstrated durability of the system and its components in engine environments.
3. No mechanical difficulties with the liquid metal regenerator were experienced even after being subjected to an uncontrolled fire in the test rig which was caused by a faulty valve dumping fuel into the hot test rig after a shutdown.
4. The prototype liquid metal pump, demonstrating principles of operation applicable to flight type pumps, performed satisfactorily throughout the tests.
5. The overall effectiveness of a liquid metal regenerator system is relatively insensitive to the circulation rate of liquid metal over a broad range of operating conditions. Beyond this range effectiveness drops sharply to zero at zero liquid metal flow.
6. Gas side fouling of the heat transfer surfaces was insignificant after 60 hours of operation at normal engine conditions. Prolonged operation with poor combustion resulted in a drop off in effectiveness and a small increase in gas side pressure drop.
7. Predicted heat-transfer performance of the liquid metal heat exchanger was not attained as a result of poor gas-flow distribution in the rig.
8. Operation of liquid metal loops for nearly 4000 hours has demonstrated long term material compatibility at engine operating temperatures.
9. The addition of cesium to NaK alloys increases the proportion of liquid-state metal at reduced temperature. Cold start-ups (-15°F) have been demonstrated with 10% cesium. Analysis indicates that retention of 98% liquidus at -65° is obtainable with 55% cesium.
10. Location of the turbine heat exchanger after the power turbine is preferred over the interstage location because of increased engine performance and because of the simplicity of installation.

3. CONCLUSION

This program demonstrated the feasibility of a liquid metal heat exchange system as a versatile, high reliability component meeting the compactness and high performance characteristics required for the Navy's regenerative turboprop engine.

4. RECOMMENDATIONS

1. Conduct long term durability tests on the regenerator system evaluated in this program.
2. Fabricate heat exchanger test modules utilizing the advanced state-of-art heat transfer surfaces developed in conjunction with this program and conduct performance and durability evaluations.
3. Fabricate and evaluate a flight weight electrodynamic liquid metal pump.
4. Conduct design and evaluation programs to establish the optimum means of providing a liquid metal heat exchange system to meet the requirements of engine start up at -65°F ambient conditions.

5. DESIGN OF HEAT EXCHANGERS

5.1.1 Design of Test Heat Exchangers

The design of the test rig heat exchangers was based on a preliminary engine cycle analysis in order to initiate early procurement of the heat transfer elements for which long delivery was expected. The turbine heat exchanger was selected as being located before the last stage of the power turbine. This choice was made prior to the ultimate determination of the turbine heat exchanger location as it allowed the test rig to be designed for the most severe operating conditions. On this basis the heat exchanger cores incorporated in the one third-sector test rig had the following specifications:

<u>Heat Exchanger</u>	<u>Compressor</u>	<u>Turbine</u>
Face Area, ft ²	.752	2.290
Number of tube rows	28	8
Fin Type	AMS 5521 (Type 310)	stainless clad copper
Fin O.D. in.	.375	.375
Fin thickness, in.	.005	.005
Core thickness, in.	.0025	.0025
Tube diameter, in.	.1875	.1875
Fins/in.	30	30
Triangular Pitch, in.	.415	.415
Tube wall thickness	.015	.015

This represented the lightest weight practical design which came closest to the required 2% pressure drop in each exchanger and to the 70% overall effectiveness for the preliminary upstream re-generator cycle.

After initiating procurement of the heat transfer elements an existing WAD computer program for the two spool turboprop engine was modified to handle both turbine heat exchanger locations. Data was obtained relative to the turbine heat exchanger location. This program showed a marginal advantage in core weight for the interstage location as higher effectiveness was approached. However, the interstage location resulted in mass flow which indicated that the gains in reduced heat exchanger weight would be offset by increased engine weight. Furthermore, mechanical design considerations indicated that extra complexity in engine construction would be incurred with the interstage location. Further, but limited, studies also indicated that the apportionment of turbine stages before and after the turbine heat exchanger would be difficult to resolve between take-off and cruise conditions. This results because of adversely changing pressure ratio requirements for the staging behind the heat exchanger.

The above considerations lead to selection of the after-turbine location as the more desirable. The established rig heat exchanger design was re-evaluated in terms of the cycle for the after-turbine heat exchanger location established by the computer program. The details of this cycle are presented in a later section. The computer program prescribed a slightly higher airflow for the compressor heat exchanger (1.2%) and a higher airflow (4.4%) for the turbine heat exchanger. The combination of higher airflow and lower inlet pressure for the turbine exchanger resulted in an increased pressure drop for this component. There was a negligible effect on the compressor exchanger pressure drop. The higher overall airflow through the engine tended to reduce the predicted overall effectiveness. The lower capacity rate ratio which resulted from the fact that the turbine airflow was increased more than the compressor airflow, tended to increase predicted overall effectiveness. The end result was that only a slight change in overall effectiveness was predicted for the two cycles. A comparison of performance at the design cruise point of 35% of normal rated power at 1500 feet altitude and 225 knots flight speed is shown below:

	<u>Preliminary Cycle</u>	<u>Selected Computer Cycle</u>
W_c , lb/sec	11.68	11.82
W_h , lb/sec	11.72	12.23
$(\Delta P/P)_{in}c$.020	.020
$(\Delta P/P)_h$.020	.036
$(\Delta P/P)_o$.040	.056
E_c	.869	.867
E_h	.788	.791
E_o	.704	.705

The liquid metal used in designing and testing the heat exchangers was an alloy consisting of 44% Na and 56% K (NaK 56).

5.1.2 Selection of Engine Cycle

It is characteristic of two spool, turbo shaft engines to have a wide range of off-design operating conditions. That is to say, there are various combinations of wheel speed and turbine entry temperatures which will result in the same shaft horsepower output. For this reason, an analysis was conducted to determine the regenerator core weights required for design conditions corresponding to those of a typical 12.6 to 1 design pressure ratio, turboshaft engine operating at several combinations of rotor speed and turbine entry temperature while producing, in each case, 35% of normal rated power at 1500 feet of altitude and 225 knots flight speed. The heat exchanger design parameters of inlet pressure, temperature

and airflow, for both the exchanger behind the compressor and the exchanger behind the turbine, were established utilizing an existing WAD computer program. The assumptions used for the engine cycle analysis are summarized below:

Altitude	1500 feet
Airspeed	225 knots
Inlet Recovery	100%
HP Turbine Mechanical Efficiency	99%
LP Turbine Mechanical Efficiency	99%
Reduction Gear Mechanical Efficiency	95%
Compressor Exchanger Core Pressure Recovery	98%
Turbine Exchanger Core Pressure Recovery	98%
Ducting Pressure Recovery	98%
Burner Pressure Recovery	98%
Turbine Exit Pressure Recovery	98%
Burner Efficiency	98%
Lower Heating Value of Fuel	18,300BTU/lb.
Nozzle Thrust Coefficient	.98
Equivalent Propeller Efficiency	80%
Overboard HP Bleed Air	1%
HP Turbine Cooling Air	1% @ 1700°F
	2% @ 1800°F
	3% @ 1900°F
	4% @ 2000°F
Turbine Entry Temperature at Normal Rated Power (TET)	2120°F
Turbine Entry Temperature at SLS-MIL Power	2200°F

For this analysis, the cores considered for the heat exchanger matrices consisted of 3/8 inch O.D., .005 inch thick, clad copper fins, spaced 30 per inch on 3/16 inch tubes placed triangularly on a pitch of .415 inches. This matrix is now considered a state-of-the-art configuration requiring little, or no, advanced technology.

The results of the analysis are presented on Figure 5.1-1 where regenerator core weight is presented versus overall effectiveness for four values of TET and different numbers of tube rows in the heat exchanger behind the compressor (N_c) and three numbers of tube rows in the exchanger behind the turbine (N_h). It is apparent that for an overall regenerator effectiveness of 70%, the designs incorporating eight tube rows in the turbine exchanger result in lighter cores, for each TET investigated, than either six or ten rows. There must of course be a whole number of tube rows, and further, mechanical design factors indicate that an even number of tube rows is desirable. Therefore, further considerations of this analysis was limited to the designs incorporating eight rows in the hot side exchanger. The higher TET's, which result in lighter

**CORE WEIGHT VS EFFECTIVENESS
ENGINE CYCLE STUDY**

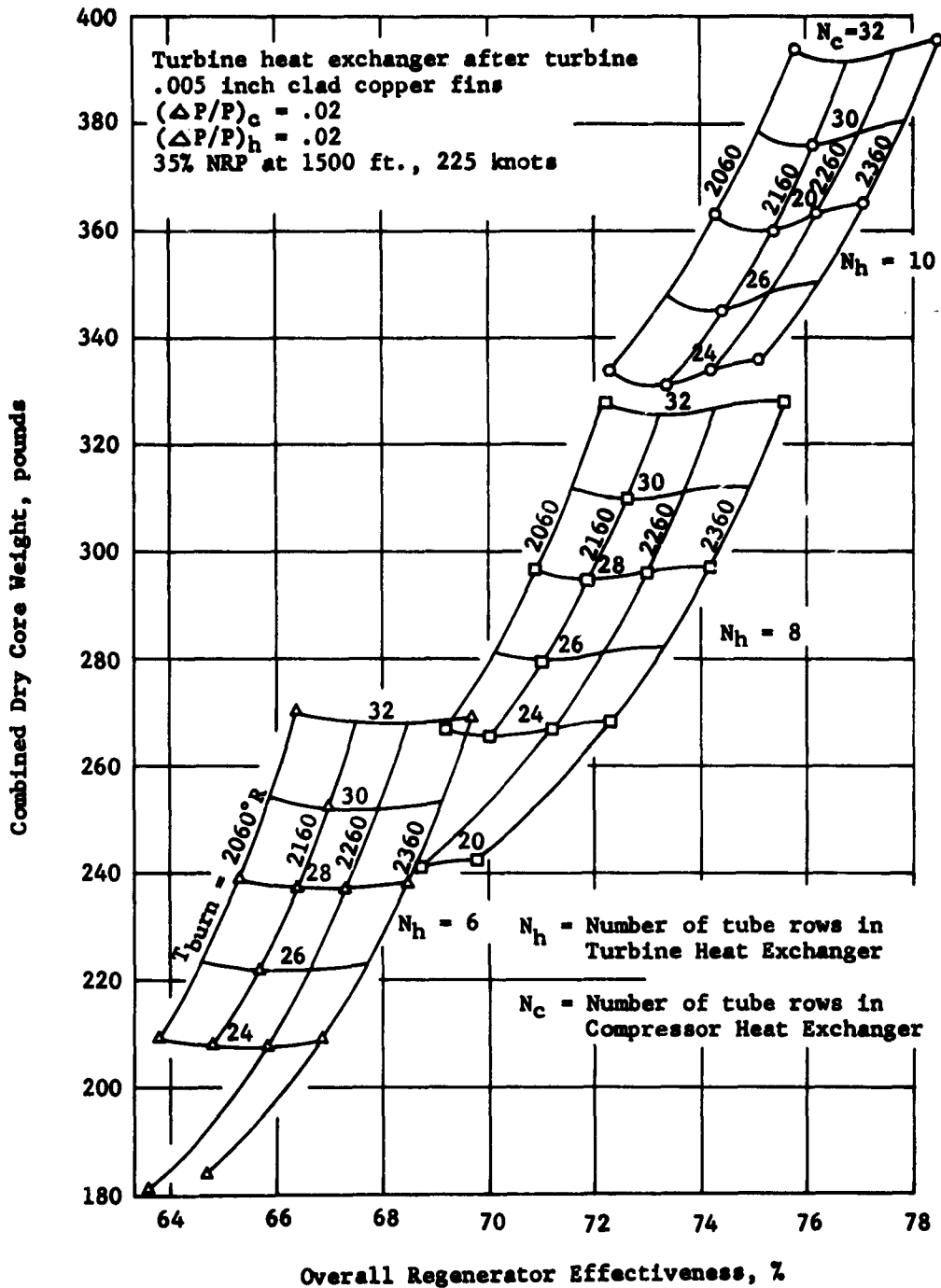


Figure 5.1-1

4777

heat exchanger core weights, result also in higher specific fuel consumption. Based on the above considerations, a turbine entry temperature of 2260°R was selected for the study engine as being the satisfactory compromise between the desirable low core weights associated with the higher TET's and the lower specific fuel consumptions associated with the lower TET's.

5.1.3 Optimization Studies

An analysis was conducted to determine the effect of varying effectiveness ratio E_h/E_c and pressure loss ratio $[(\Delta P/P)_c/(\Delta P/P)_H]$ on heat exchanger core weight. The analysis was done for a typical 12.6 to 1, design pressure ratio, two spool turboprop engine operating at 1500 feet at 35% of normal rated power with a turbine entry temperature of 1600°F. The core consisted of the optimum .003 inch thick aluminum bronze fins described in the separate report CTR.00-272. The overall regenerator effectiveness was maintained constant at 70 percent and the overall pressure drop (defined as $[(\Delta P/P)_c + (\Delta P/P)_H]$) was held constant at .04.

The results of this analysis are presented in Figure 5.1-2 in terms of combined core weight (including NaK) versus effectiveness ratio for five pressure drop split ratios. They can be summarized as follows:

1. For each pressure drop split ratio, the minimum combined core weight invariably occurs at effectiveness ratios near unity.
2. As the pressure drop split ratio increases from .05 to 19.0, optimum effectiveness ratio decreases from 1.02 to .93.
3. Between the pressure drop split ratios of .33 and 1.0, there is no appreciable change in optimum core weight. Outside these limits, the weight increases by 12% for .05 ratio, 6% for 3.0, and 24% for 19.0.

In general, it can be said that a considerable area is available both in pressure drop split ratio and effectiveness ratio within which the heat exchanger core weight will not be seriously effected. If the pressure drop split ratio is kept between .33 and 1.5 and the effectiveness ratio between .91 and 1.02, the weight of the core will be no more than 6% more than the optimum weight.

CORE WEIGHT VS EFFECTIVENESS RATIO

Turbine heat exchanger after last turbine stage
 .003 aluminum bronze fins
 $(\Delta P/P)_c + (\Delta P/P)_h = .04$
 35% NRP at 1500 ft., 225 knots
 Turbine entry temp. = 1500°F

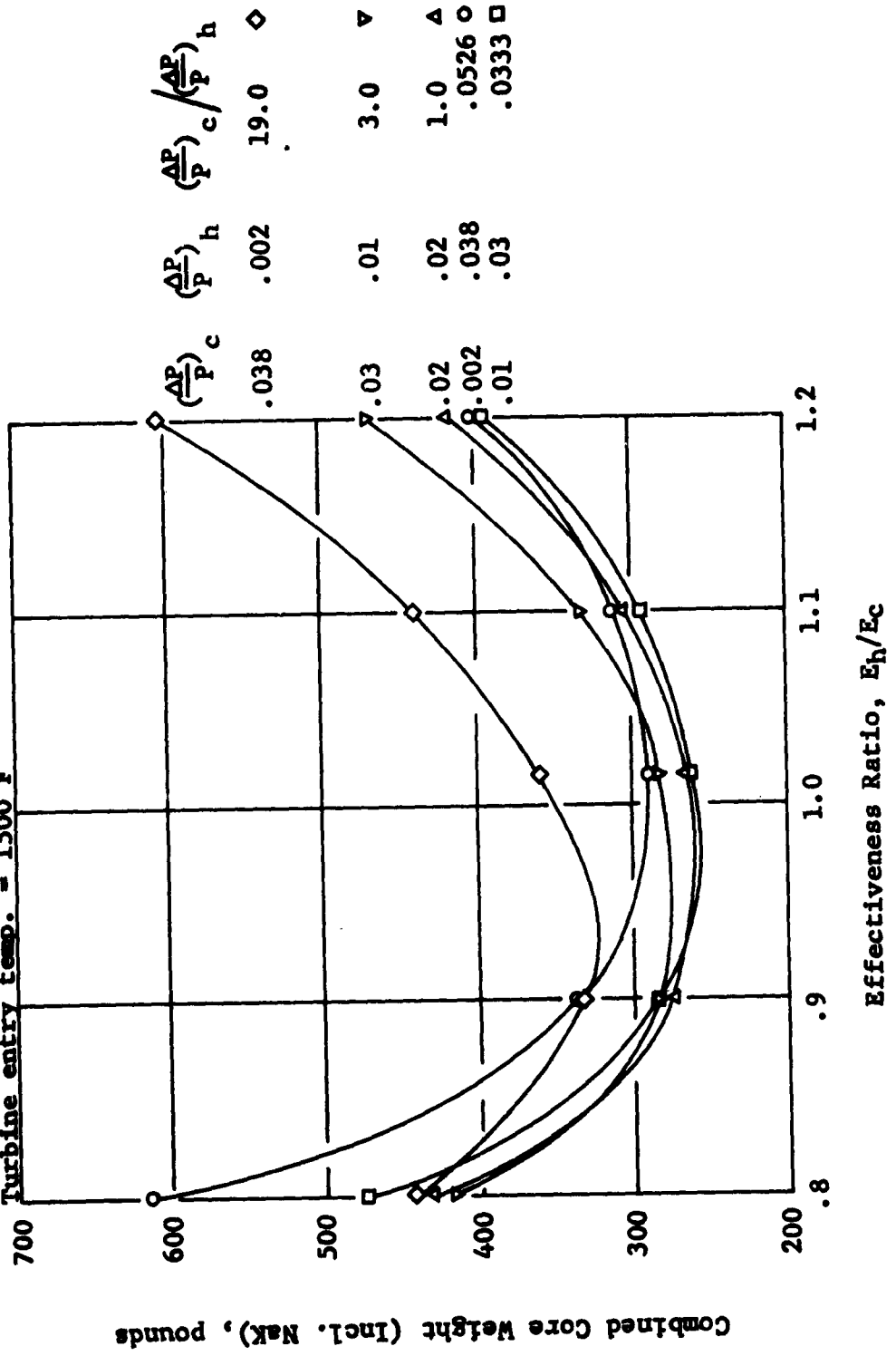


Figure 5.1-2

5.1.4 Design of Study Engine

Two locations were considered for the turbine heat exchanger; 1) located completely to the rear, behind the last turbine stage, and 2) located upstream of the last turbine stage. The heat exchanger weights versus effectiveness for the 12.6 to 1 design pressure ratio engine at the 1500 ft. 225 knot cruise condition with an 1800°F turbine entry temperature and the regenerator located in the above two positions, were compared for the case of equal pressure losses (2%) in each exchanger. This analysis utilized the optimum aluminum bronze fin configuration previously established. The results are presented on Figures 5.1-3 and 5.1-4. The weight of the active finned tube core (not including NaK, return bends or other supporting hardware) is presented versus effectiveness for different numbers of tube rows in each exchanger. Although, for clarity in presentation, curves are shown representing constant numbers of tube rows in the hot exchanger, only the points themselves represent practical designs. The comparison between the upstream and aft regenerator designs must, therefore, be made on a point-for-point basis rather than on the relative positions of the curves. On this basis, it can be seen that for an overall effectiveness near 70%, the aft regenerator design with 8 rows in the hot exchanger and 32 rows in the cold exchanger results in a combined heat exchanger core weight which is 13 pounds heavier (220 vs 207) than the upstream regenerator design with 10 rows in the hot exchanger and 28 rows in the cold exchanger. Inasmuch as, there is not significant difference in specific fuel consumption for the two concepts and considering that the upstream regenerator design would require additional ducting and a longer main shaft, it is felt that the aft design is most applicable for the engine. This cycle incorporated the assumptions listed previously and resulted in the following characteristics at 1500 feet and 35% of normal Rated Power:

Compressor Pressure Ratio	6.136
Turbine Entry Temperature	1800°F
Compressor Exchanger Air Flow	11.818 lb/sec
Turbine Exchanger Air Flow	12.228 lb/sec
Compressor Exchanger Inlet Temperature	490°F
Turbine Exchanger Inlet Temperature	1105°F
Compressor Exchanger Inlet Pressure	184.7 in. Hg Abs.
Turbine Exchanger Inlet Pressure	30.87 in. Hg Abs.
L.P. Compressor Polytropic Efficiency	72%
H.P. Compressor Polytropic Efficiency	88%
Nozzle Pressure Ratio	1.045
Equivalent Shaft Horsepower	1388 HP

**CORE WEIGHT VS EFFECTIVENESS
STUDY ENGINE**

Turbine heat exchanger after last turbine stage
 .003 aluminum bronze fins
 $(\Delta P/P)_c = .02$
 $(\Delta P/P)_h = .02$
 35% NRP at 1500 ft. 225 knots
 Turbine entry temp. = 1800°F

Sym.	N_c
○	24
□	28
△	32

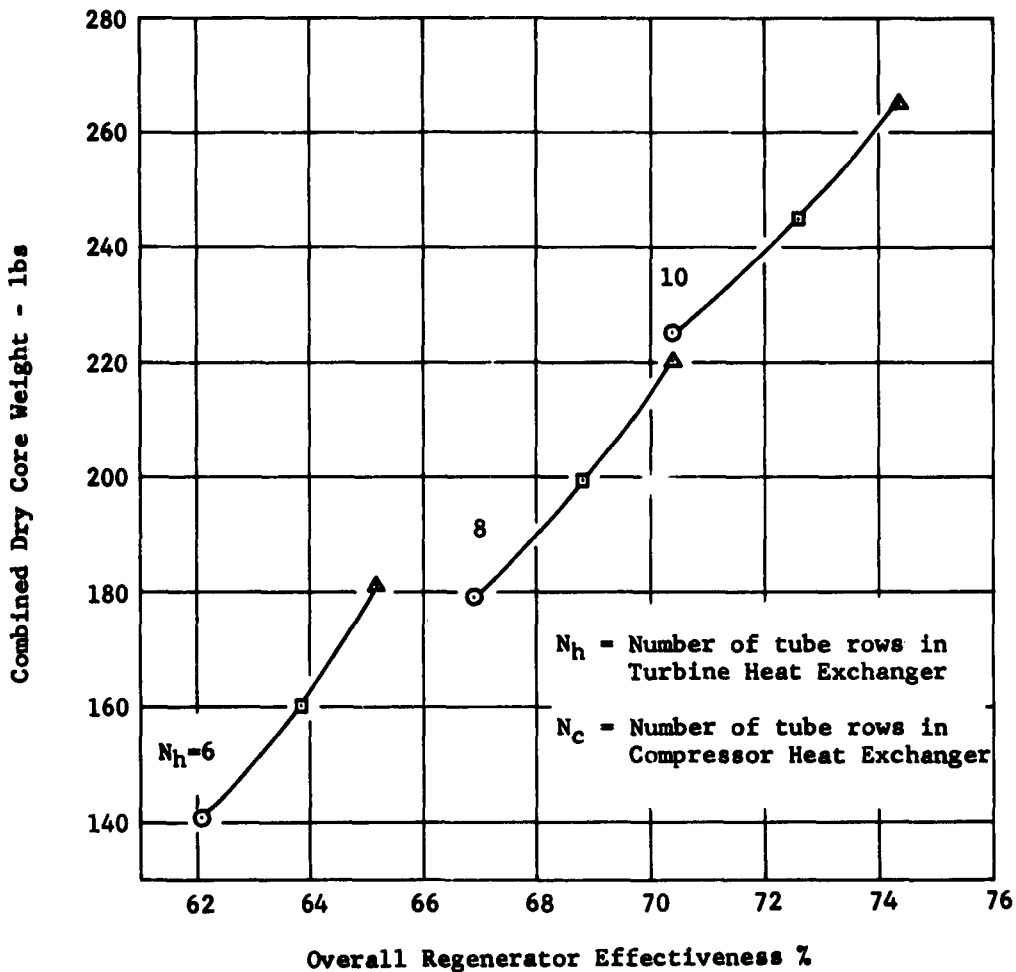


Figure 5.1-3

**CORE WEIGHT VS EFFECTIVENESS
STUDY ENGINE**

Turbine heat exchanger upstream of last turbine stage
 .003 aluminum bronze fins
 $(\Delta P/P)_c = .02$
 $(\Delta P/P)_h = .02$
 35% NRP, at 1500 ft, 225 knots
 Turbine entry temp. = 1800°F

Sym.	N_c
○	24
□	28
△	32

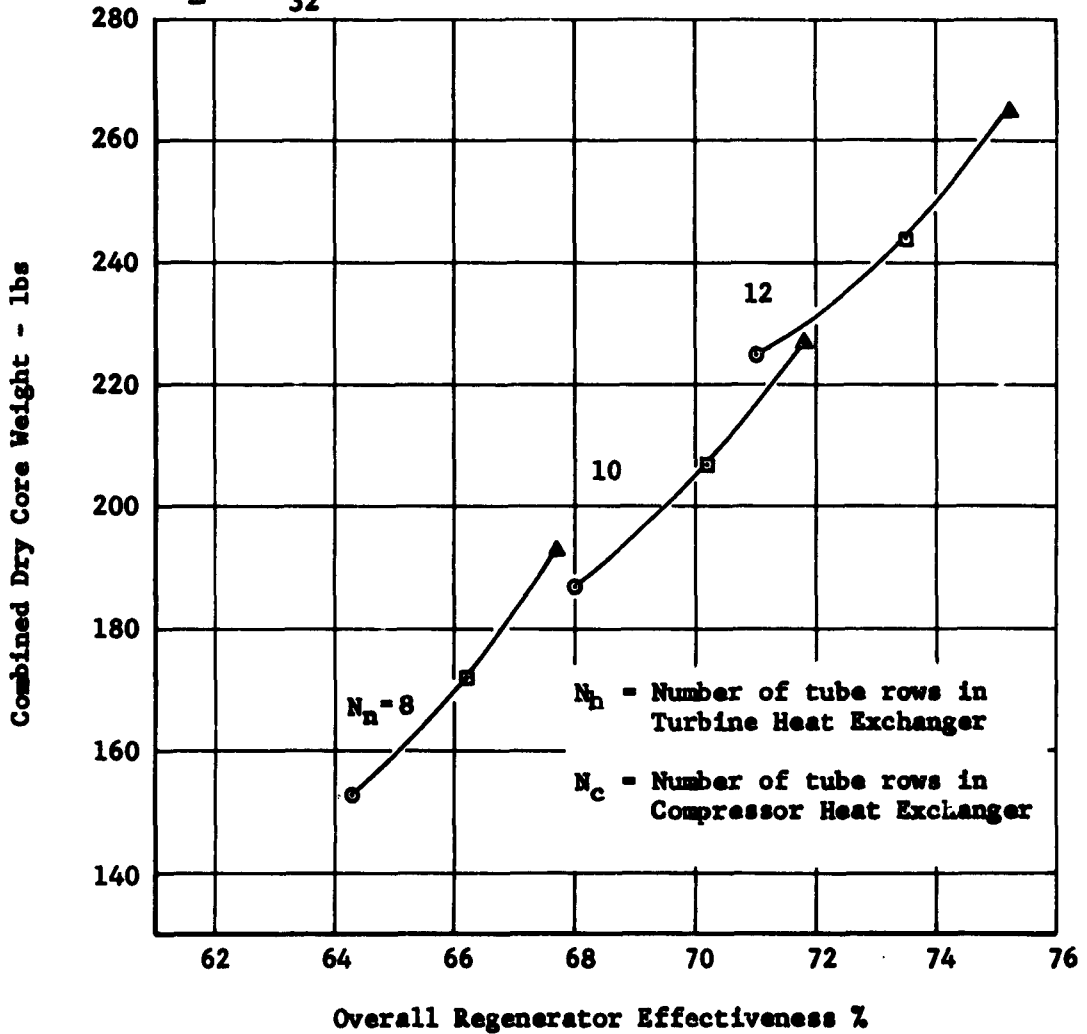


Figure 5. 1-4

The balanced pressure drop design resulted in a cold side heat exchanger face area which was somewhat larger than desirable. Therefore, the cold side pressure drop was increased to 2.25% and the hot side reduced to 1.75%. This results in the same combined pressure drop of 4% to which engine performance is sensitive. As expected from the results of the optimization study on effectiveness split and pressure drop split, the combined core weight was not appreciably affected. The final regenerator design incorporated in the study engine had the following specifications:

	<u>Cold Exchanger</u>	<u>Hot Exchanger</u>
Face area, ft ²	2.068	9.20
Number of tube rows	32	8
Component: Core weights, Dry, Lbs.	105	116
effectiveness, %	85.0	80.0
pressure drop, $\Delta P/P_{in}$.0025	.0175
Overall: Core weight, Dry, Lbs.		221
effectiveness, %		70.7
pressure drop, $\Delta P/P_{in}$		4.0

It can be seen that the effectiveness split of $E_h/E_c = .93$ (which was established by the requirement for whole numbers of tube rows) is within the limits of .91 to 1.02 which was established in the optimization study on effectiveness and pressure drop splits.

5.1.5 Take-Off Considerations for Study Engine

The configuration discussed previously had been designed for a specific pressure loss at the 35% power at 1500' cruise condition. At take off conditions, unless the hot exchanger is bypassed, this pressure loss would be higher. The design selected for the study engine for instance, which has a total $\Delta P/P$ of .04 at cruise, would have .062 combined $\Delta P/P$ at take off.

In view of these facts, an analysis was conducted to determine the effect on the study engine core weight resulting from designing the heat exchangers for .04 overall pressure drop at take off conditions rather than at the 35% power cruise conditions.

The analysis showed that this approach would result in little or no increase in the overall regenerator system weight and, based on the face areas of the cold exchangers, could be accomplished within approximately a 30 inch maximum engine diameter envelope.

The primary advantage of this system would, of course, be the elimination of the bypass. In addition, however, by permitting the

regenerator to operate at all power settings, it would make possible lower SFC's at higher power cruise points such as the 75% power at 10,000 feet, as required for the AEW mission.

The results of this analysis are summarized in detail in Table 5.1-5 where the performance weight and face areas of two possible designs giving 4% overall pressure drop at take off (Configuration 1 and 2) are compared to the original design (Configuration 3) yielding 4% overall pressure drop at the 35% power cruise condition. Performance is shown for operation at take off, 35% power cruise at 1500' and 75% cruise at 10,000 feet.

Configuration 1 is for balanced pressure drop at take-off resulting in unbalance at the 35% cruise condition. The second configuration incorporated unbalanced pressure drops at take-off which resulted in balanced pressure drops at the 35% cruise condition. Both configurations are the designs which came closest to the desired 70% overall effectiveness at the 35% power cruise condition and incorporated practical numbers of tube rows.

It is readily apparent that the second configuration is the better of the two alternate designs since it not only yields the lowest dry core weight, but also results in the lowest overall pressure drop at the 35% power cruise condition. In addition, the face area of the hot gas exchanger behind the turbine has been increased from 9.2 (for the design at cruise) to only 11.34 square feet compared to 14.16 square feet for the first configuration.

In view of the complexity of a bypass system and considering the results of this analysis, it appears quite feasible that a regenerator could be designed without bypass, with no more than 4% overall pressure drop at take off and with little or no sacrifice in system weight compared to the bypassed configuration.

5.2 Mechanical Design of Test Heat Exchangers

5.2.1 Compressor Heat Exchanger

The requirements of relatively low frontal area and large number of tube rows for the compressor heat exchanger was best satisfied by an axial gas flow arrangement. The heat exchanger form was made annular to obtain an open central core to accommodate other engine components. The finned tube serpentine heat transfer elements were arranged so that the hot liquid metal entered the serpentines at the air discharge side and moved in a counter-flow fashion in respect to the air to discharge at the air inlet side. The plane of the serpentine was bent to an involute shape to obtain uniform tube

Comparative Regenerator Designs - Study Engine

	Alternative 1.		Alternative 2.		Original Design	
	(1) 35% Cr. @ 1500'	.04 @ T.O. 75% Cr. @ 10,000'	(2) 35% Cr. @ 1500'	.04 @ T.O. 75% Cr. @ 10,000'	(3) 35% Cr. @ 1500'	.04 @ 35% 75% Cr. @ 10,000'
($\Delta P/P$) _c	.02	.024	.01	.012	.019	.0225
($\Delta P/P$) _h	.02	.008	.03	.012	.045	.0175
($\Delta P/P$) _o	.04	.032	.04	.024	.064	.04
$E_o, \%$	62.4	69.4	64.2	70.7	64.4	70.7
M_c	24		24		32	
M_h	8		8		8	
A_{fc}, FT^2	1.710		2.509		2.068	
A_{fh}, FT^2	14.16		11.34		9.20	
W_o, Lb	244		239		221	

TABLE 5.1-5

spacing throughout the full annular gas passage. The fin tube serpentines terminated fore and aft in circular arc headers external to the gas stream.

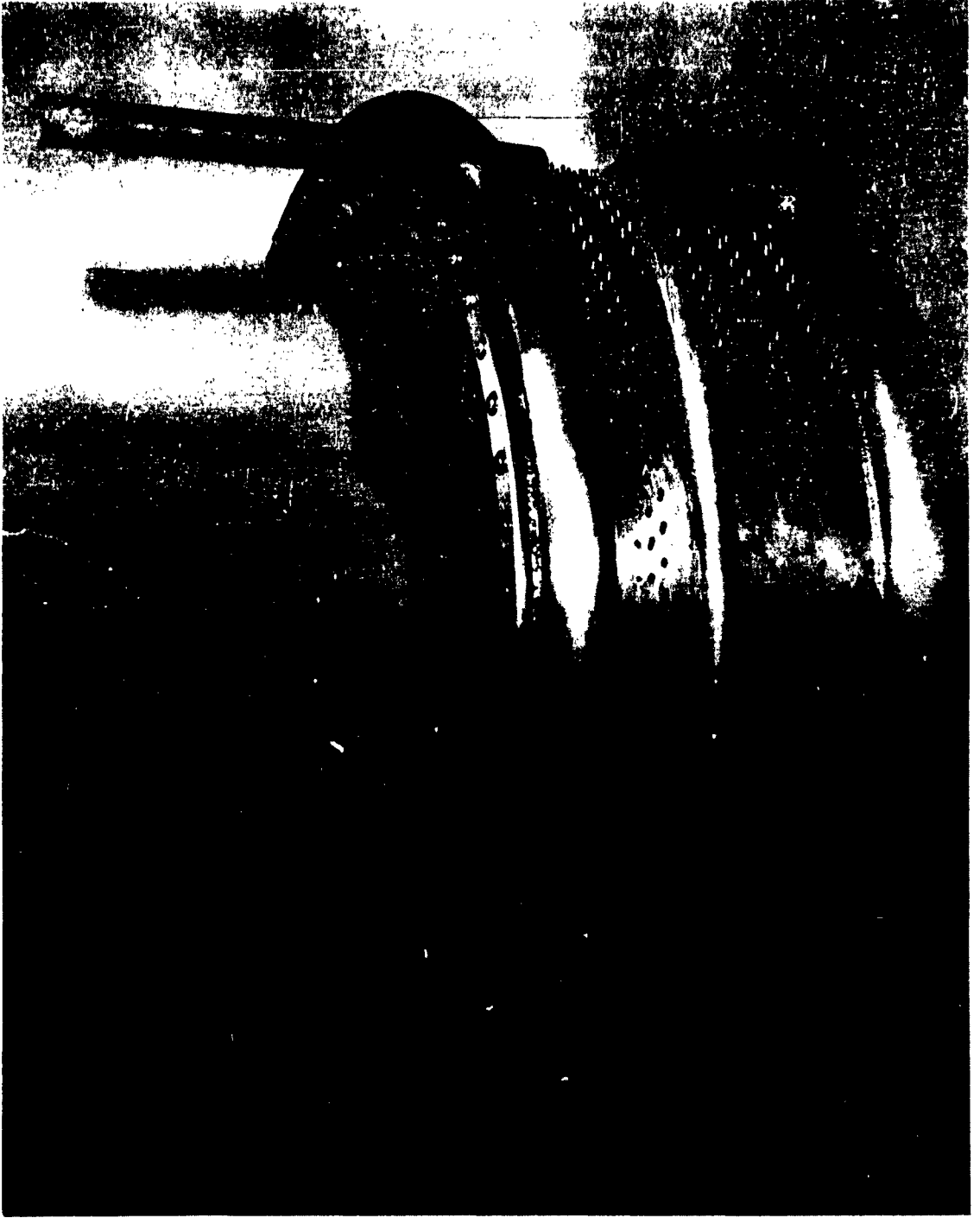
Inner and outer circumferential shells confined the gas stream and supported the fin tube serpentines throughout their length. The outer shell was supported from the front header which in turn was supported by a flanged element for mounting to the test rig. The rear liquid metal header was allowed to float in respect to the outer shell and was supported by the finned tube serpentines. This header mounting permits large relative thermal expansion which could occur should hot liquid metal suddenly enter a relatively cool heat exchanger. Such conditions would occur if the turbine heat exchanger were placed interstage of the power turbine and liquid metal circulation had been stopped to achieve a thermal by-pass and again started.

A design objective of the heat exchangers was to use a sectored construction to facilitate mounting the liquid metal regenerator to an engine. For purposes of evaluation the full heat exchanger was considered as being made up of three 120° sectors. The test heat exchanger was made as a 120° sector and had air confining side walls made to the shape of the involute tubes, Fig. 5.2-1. These walls were made solid and heavier than would be required in a full complement of heat exchanger sectors where no need would exist for lateral confinement of the air.

The extreme flexibility of the serpentines required that they be supported at the return bends to minimize vibration and to withstand aerodynamic and inertia loads. It was essential that the supports produce no chaffing on the relatively thin walls of the tubes at the return bends. Structural and weight considerations led to the selection of projecting pins brazed to the return bends to engage the supporting shells, Fig. 5.2-2. Projecting baffles were provided on the supporting shells in between groups of return bends to limit air flow over the unfinned return bends. Some air flow in this area is desirable to utilize the return bends as heat transfer surface and to provide heat to the return bends for rapid thawing of liquid metal particles during cold start conditions.

The headers were designed in concentric halves to provide access for welding the tubes of the serpentine heat transfer elements. All tube welds were made from the liquid metal side, Fig. 5.2-3. The inner header was machined from a solid ring forging. Consideration was given to spinning the inner header from a flat ring which appeared attractive from a production viewpoint. However,

COMPRESSOR HUB AT EXHAUST
120° Sector



5617

Figure 5.2-1

MOCK UP OF COMPRESSOR HEAT EXCHANGER SHOWING
PIN SUPPORTS AND BAFFLES



5015

Figure 5.2-2

COMPRESSOR HEAT EXCHANGER
Tube to Header Welding Fixture

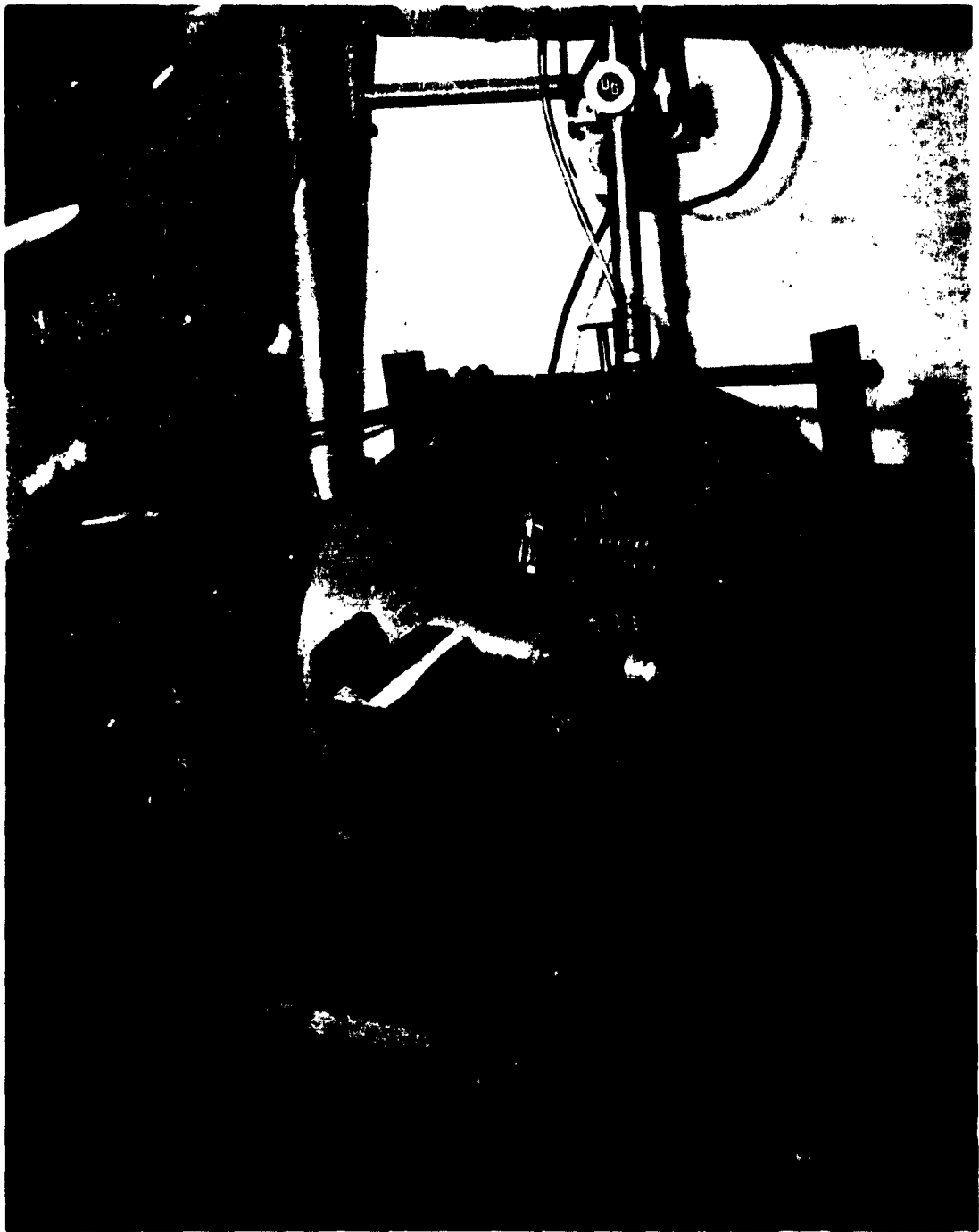


Figure 5.2-3

5018

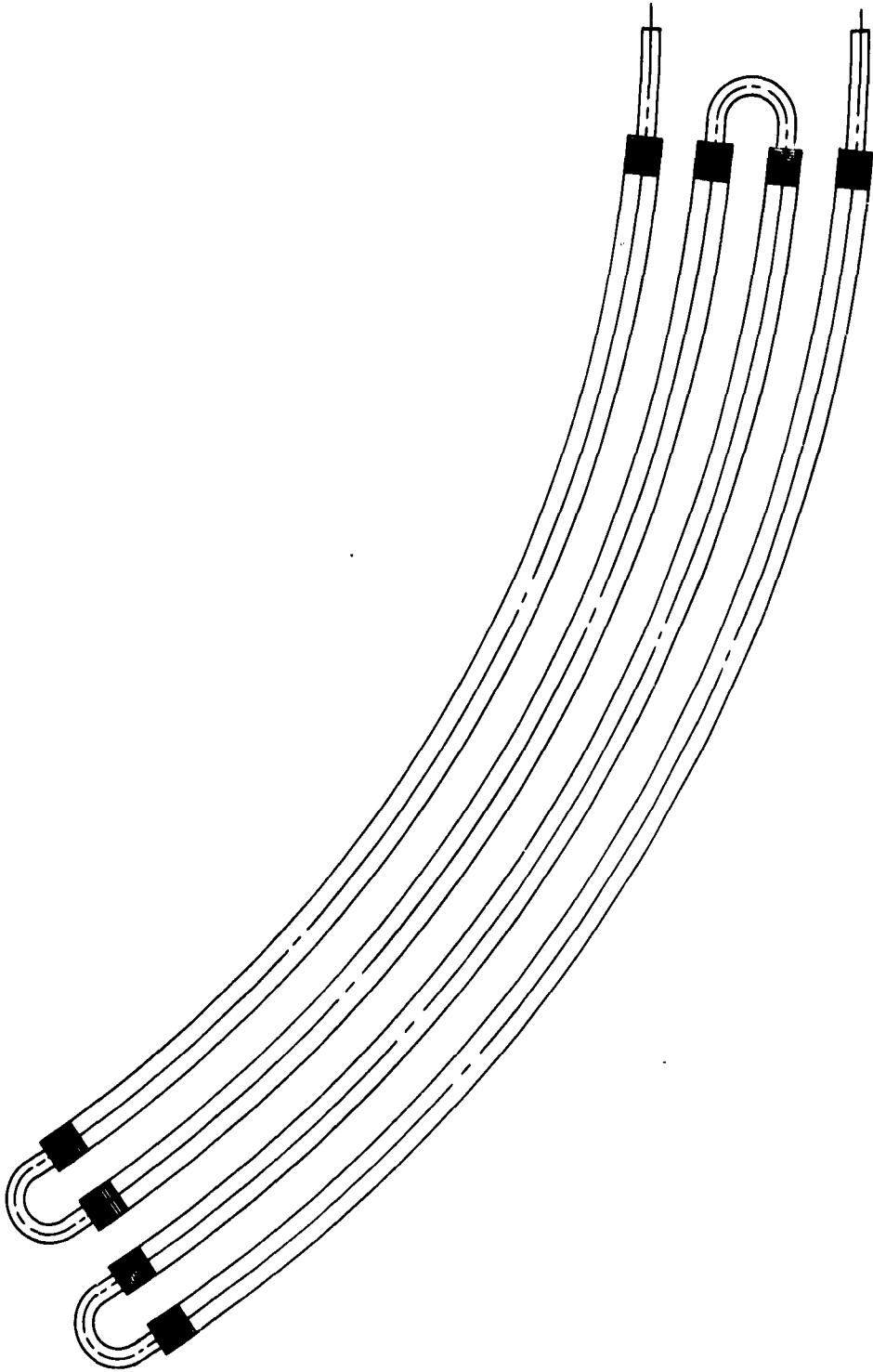
the time and cost to develop tooling could not be justified. The outer half of the headers was cut from a bent tubular ring. The header halves were joined by inert gas welding.

5.2.2 Turbine Heat Exchanger

High face area requirements and few tube rows determined that the basic configuration of the turbine heat exchanger be that of a hollow cylinder through which gas flowed radially outward. Liquid metal was made to flow radially inward through finned tube serpentines to obtain counterflow heat transfer. Two basic arrangements of the finned tube serpentine were considered for the turbine heat exchanger. The serpentines could run fore and aft as elements of the cylinder or could run circumferentially to form sections of the cylinder. Evenly spaced serpentines in the fore and aft concept produced a circumferential divergence in tube spacing which increased with each successive outward row of tubes. The increase in tube spacing resulted in significantly reduced performance. Bundling the tubes in rectangular packages would have provided uniform tube spacing to maintain heat exchanger performance. However, such packages would have required intermediate baffles which would have added weight to the systems and would have had an unpredictable effect on performance. Header construction, also, would have been more complicated.

The circumferential serpentines were chosen since uniform tube spacing could be maintained throughout the full heat exchanger. The headers ran fore and aft and were shorter and lighter than the circumferential headers required for the fore and aft oriented serpentines. The circumferential serpentines resulted in a bowed configuration which offered structural advantages and good vibration control. Figure 5.2-4 depicts such a configuration which is readily supported against stresses arising from vibration and "g-loading" associated with linear and rotational accelerations. Initial fabrication studies indicated the feasibility of fabricating bowed serpentines. However, lack of experience in production forming of bowed serpentines and the necessity to develop tooling made timely procurement questionable. Straight serpentines were used with a fore and aft header arrangement typical of a bowed serpentine heat exchanger. The straight serpentines were mounted to form one-third of a hexagon with a midpoints of the sides tangent to the circle that would have been formed by the bowed serpentines, Fig. 5.2-5. Nesting the serpentines to obtain a triangular pitch configuration required that the eight row depth of the heat exchanger be achieved by a staggered arrangement of four pass serpentines. Performance studies showed that a four pass cross-counterflow arrangement deviated from full-counterflow performance to the extent

BOWED HEAT TRANSFER ELEMENT



5823

Figure 5.2 4

TURBINE HEAT EXCHANGER



Figure 5.2-5

6431

that the size of the heat exchanger had to be increased. The increased size, prorated to a full 360° liquid metal regenerator, amounted to a 12 lbs. increase in total weight. Achievement of eight pass cross-counterflow arrangement which closely approaches full-counterflow performance is possible by offsetting the return heads of the serpentine to obtain 8 rows (Figure 5.2-6). Although feasibility was demonstrated, this configuration was abandoned because of possible delays in procurement.

The serpentes were supported by projecting pins brazed to the return bends. These pins engaged supporting plates which gave lateral restraint but permitted longitudinal movement for thermal expansion, Fig. 5.2-7. The supporting plates had projecting baffles interspaced between return bends to permit limited flow across the return bends to achieve additional heat transfer and to provide a warm gas supply for cold start conditions.

The headers were each made in three longitudinal sectors. Two sectors were opposite pairs and were drilled to receive the tube ends of the serpentes. Tube to header welding was done from the liquid metal side. Sub-assemblies of the heat exchanger consisted of two halves with serpentes welded to header sectors, Fig. 5.2-8. In final assembly the header sectors containing the tubes were welded from the liquid metal side. The third sector which closed the header was welded from the gas side. All header sectors were formed to circular shapes from flat stock.

5.3 Study Engine - Mechanical Design

A liquid metal regenerator system was designed subsequent to the test rig design to represent latest thinking on arrangement and to include findings on advanced heat transfer elements demonstrated as feasible in a companion investigation. Figure 5.3-1 depicts the liquid metal regenerator system included in an engine arrangement representative of the engine used to establish state conditions for the test heat exchangers. The turboprop study engine is a two spool high pressure ratio (12.6:1) engine with a regenerator system effectiveness of 70% and a maximum engine diameter of 30.5 inches. The compressor regenerator air flow is axial and the turbine regenerator air flow is radial inward.

Through experience, the finned tube serpentine has been selected as the most attractive design for the extended surface heat transfer element possessing the qualities necessary for aircraft applications. The construction lends itself to being durable, light weight, and easily manufactured with sound thermal bonds of leakproof construction.

OFFSET RETURN BEND SERPENTINE

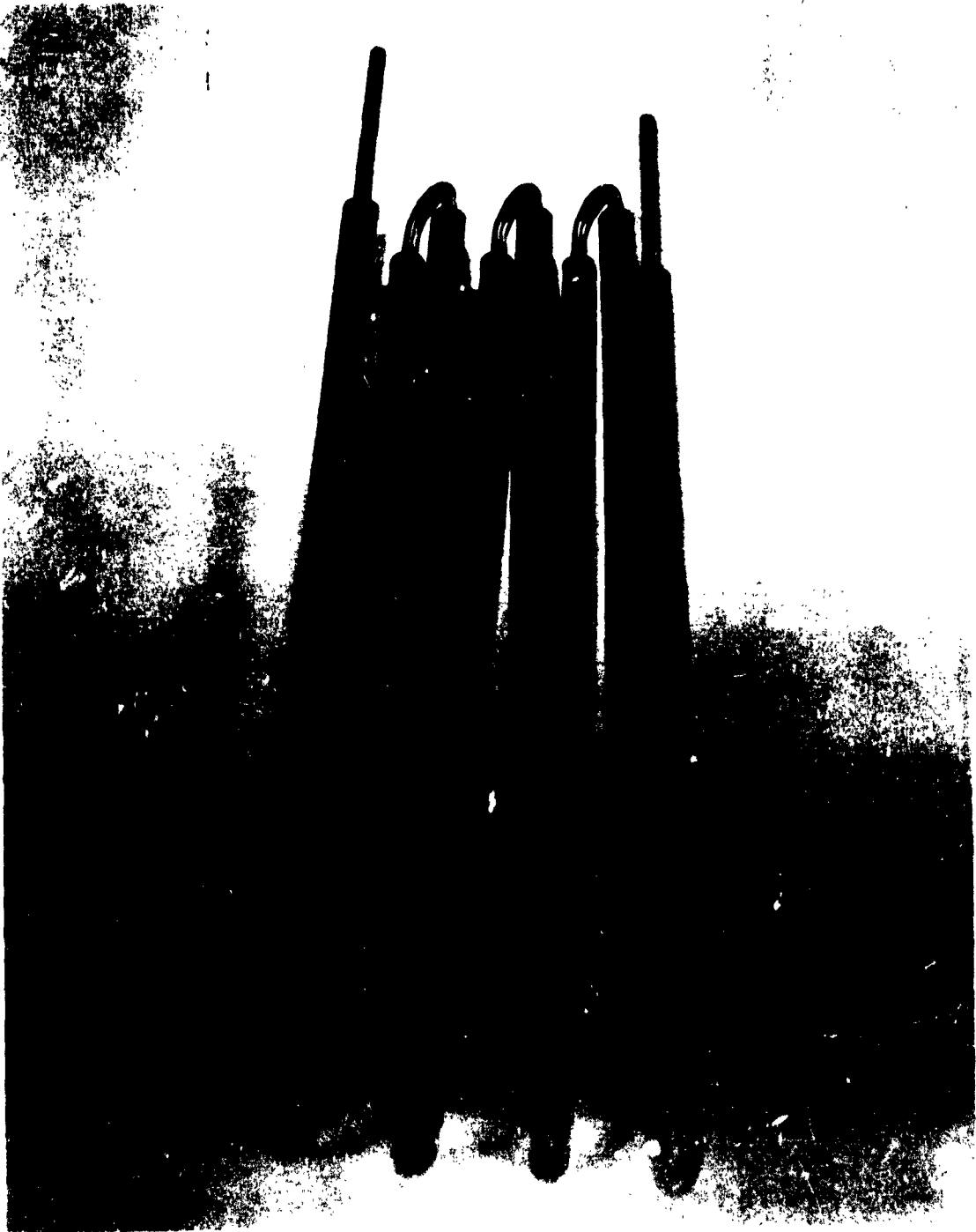


Figure 5.2-6

9616

TURBINE HEAT EXCHANGER - TUBE SUPPORT

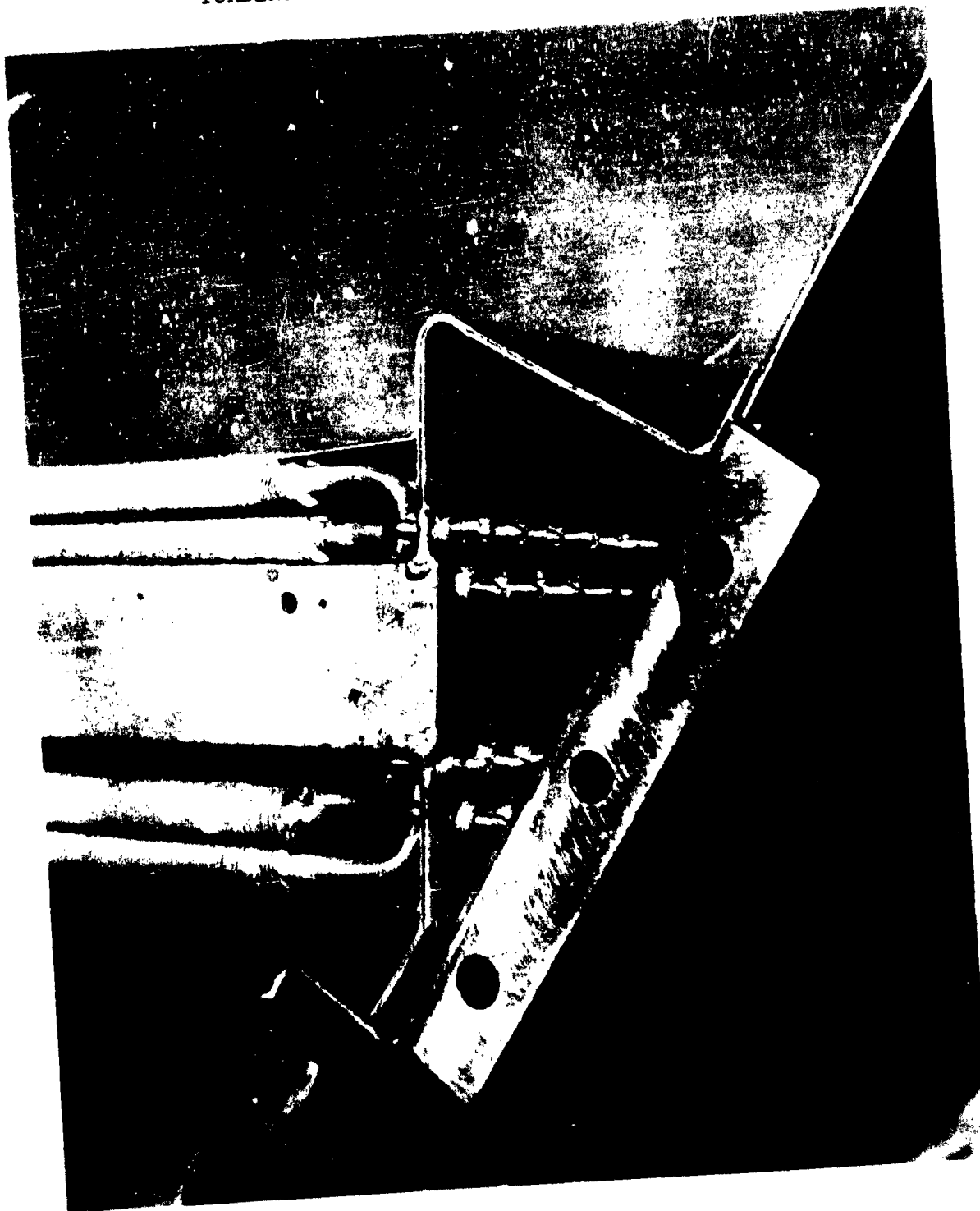


Figure 5.2-7

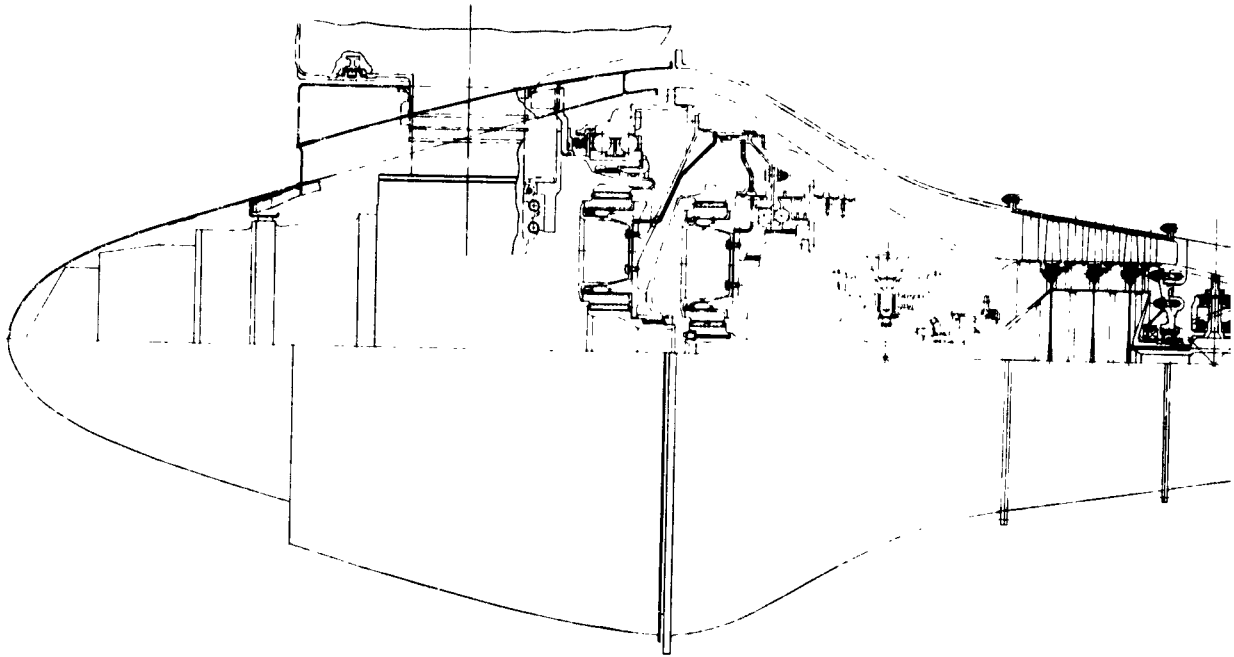
5814

TURBINE HEAT EXCHANGER - SUB ASSEMBLIES



Figure 5.2-8

5633



**CONFIGURATION STUDY
3750 H.P. LIQUID METAL REGENERATED
TURBOPROP ENGINE**

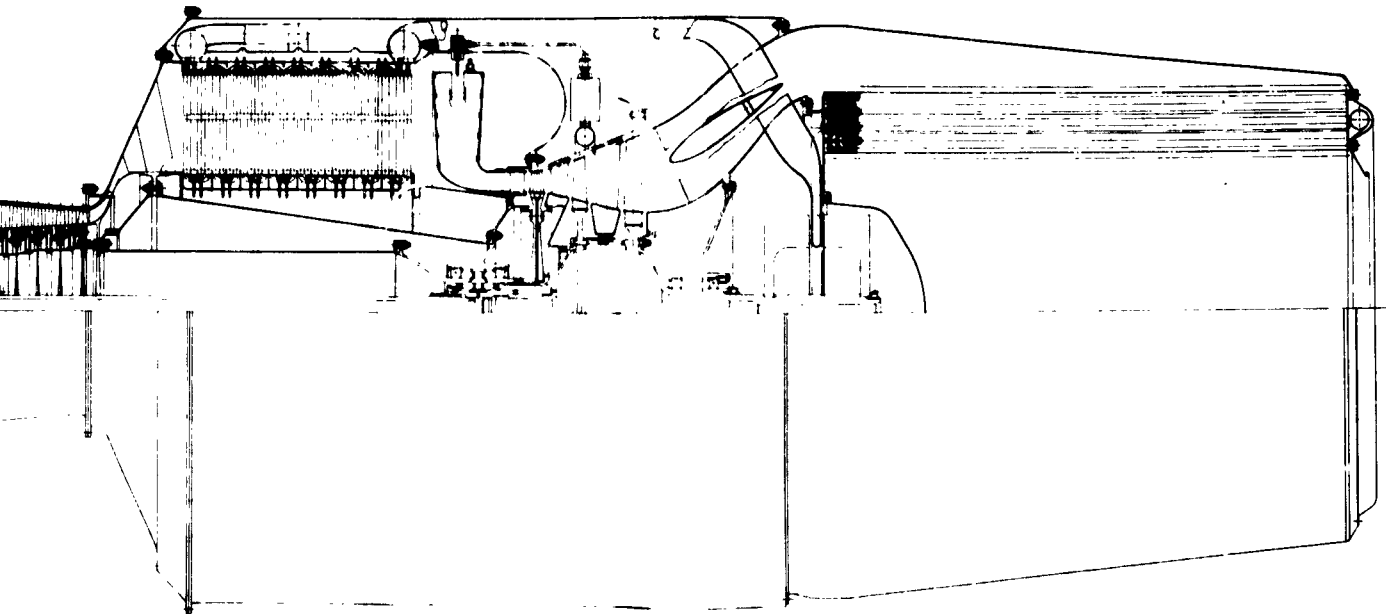


Figure 5.3-1



The sectored construction of the liquid metal regenerator system allows for servicing, inspection and removal of the heat exchanger units complete with pumps and lines without breaking a line or draining the system. The sector concept is shown, schematically, in Figure 5.3-2.

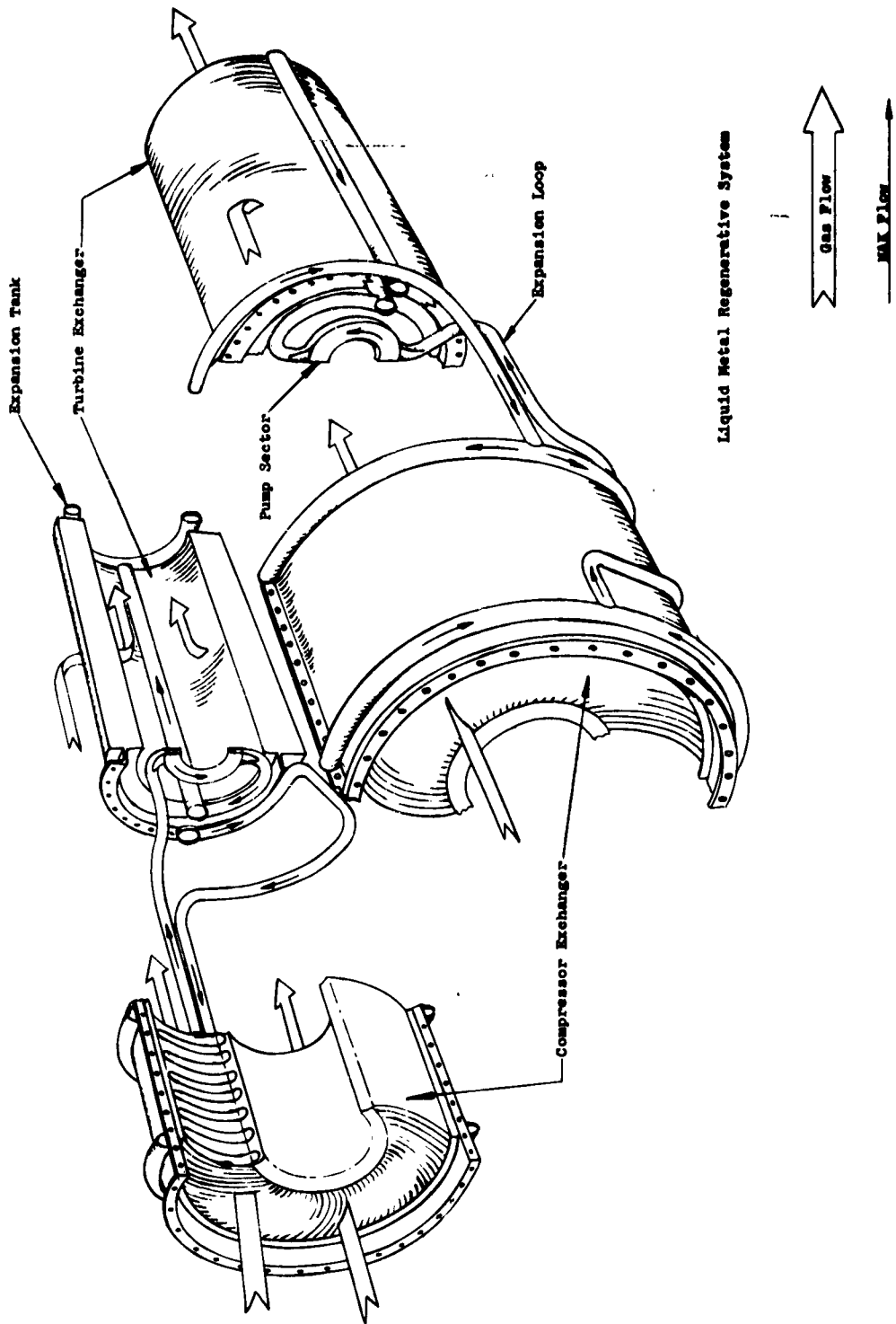
The reduction gear box is a two-stage planetary reduction with a 17.5 to 1 reduction ratio. The planet carrier is fixed and the ring gear is the output gear (in both stages). There are three planet gears in the first stage and five planet gears in the second stage. The compressor is a two spool nine stage axial flow compressor, pressure ratio 12.6:1, with a mixed flow radial discharge, final stage. The low pressure compressor is a three-stage unit with solid disks and pin supported blades. The high pressure compressor is a six-stage unit with bored discs, pin supported blades and a welded rotor shaft. The last stage of this compressor is a mixed flow radial discharge design providing improved compressor heat exchanger inlet diffuser performance.

The compressor heat exchanger is an axial air flow exchanger of counter flow design which is made in two 180° units. The exchanger consists of thirty-two counterflow rows with sixteen rows in each involute serpentine element. The involute serpentine elements are fusion-welded to the circumferential manifolds. The manifolds are located at the O.D. of the exchanger, one at the entrance and one at the exit plane. The elements are supported by means of pins brazed to each return bend. The pins extend through inner and outer shells, thus providing for thermal expansion. The outermost shell is a pressure shell which eliminates the need for seals around the liquid metal loop tubing.

The combustion chamber (located at the exit of the compressor heat exchanger) is a radial in-flow burner with conical walls. This unit has eighteen vaporizers and eighteen primary air cups equally spaced on the outer cylindrical surface (head plate). The main dilution air is used to cool the combustion chamber walls and is introduced at various critical locations.

The high pressure turbine is a single-stage turbine with transpiration cooled rotor and stator blades. The blades and disks form a welded assembly to provide cooling air passages and to eliminate cooling air leakage. Cooling air is supplied to this manifold, formed by the blades and disks, through radial holes originating at the disk bore. The low pressure turbine is a two-stage turbine with fir-tree blade attachment and solid rotor disks.

The turbine heat exchanger is a short radial inflow heat exchanger



4788

Figure 5.3-2

having high effectiveness and low pressure drop. This exchanger has a low loss inlet diffuser designed to give improved exchanger inlet flow distribution. The two 180° sectors of the heat exchanger consist of eight counterflow rows with four rows in each bowed serpentine element. The serpentine elements are fusion-welded to axially-aligned manifolds. Each pair of manifolds is located at the mid-circumferential span and has bowed serpentine elements extending from each side. Supports are provided at 45° intervals to provide additional vibration damping. The individual tube elements are allowed freedom to expand without causing large stresses in the tube-to-manifold joints. This is accomplished by brazing pins at the center of each return bend. The pins extend through holes in a support plate which indexes the elements but does not hinder their thermal expansion. Additional flexibility for thermal expansion is provided by allowing the manifolds to float.

The compressor and turbine heat exchanger units are inter-connected by a pump and piping network to form the regenerator system. The pump shown is an electrodynamic type, and consists of an engine driven magnetic rotor which straddles a semi-circular pump cell carrying the liquid metal. The important advantages of this type of pump are simplicity, no seal requirements, and no mechanical connections in the liquid metal circuit. Because of the pump arrangement, the exchanger units can be removed from the engine without breaking the liquid metal lines. This feature makes possible the design and fabrication of the regenerator system in sectors.

The pump is housed in a container mounted to the rear main bearing housing at the forward edge of the turbine exchanger. The pump supply line comes from the compressor exchanger down the aft section of the rear main bearing strut, and thus to the pump. The pump is connected directly to the engine power turbine shaft and is cantilevered from the rear bearings.

The liquid metal expansion tank is located in the relatively cool area at the rear end of the turbine exchanger and is connected to the turbine heat exchanger inlet manifold.

The study engine regenerator system weights are summarized in Table 5.3-3.

The core weights are based on advanced heat transfer elements made of .003" aluminum bronze fins .375" O.D. spaced 30 per inch on .188" O.D. tubing having .015" wall thickness. The core weight can be reduced 38 lbs. by using .010" tubing for the heat transfer elements which now seems feasible. Applying this weight saving to the weight of the study engine regenerator results in a final weight of 348 lbs. for the complete regenerator system.

Regenerator Component Weights - Study Engine

Compressor Exchanger

Active Core	105	
Braze	5.4	
Return Bends	7.8	
Pins	5.5	
Headers	12.14	
Forward Outer Flange	3.1	
Outer Support	4.12	
Outer Pin Support	7.0	
Rear Outer Flange	4.45	
Inner Support	<u>4.86</u>	
Total		159.37

Turbine Exchanger

Active Core	116	
Braze	6.3	
Return Bends	6.5	
Pins	2.43	
Clips	3.86	
Headers	8.66	
Pin Support and Baffle Ass'y	5.23	
Front Support	5.92	
Rear Support	<u>4.73</u>	
Total		159.63

Liquid metal		27
Liquid metal loop and expansion tank		15.0
Liquid metal pump		<u>25.0</u>
Total		386

Potential Weight Reductions		<u>38</u>
Total		348

TABLE 5.3-3

6. FABRICATION OF HEAT EXCHANGERS

6.1 Heat Transfer Elements

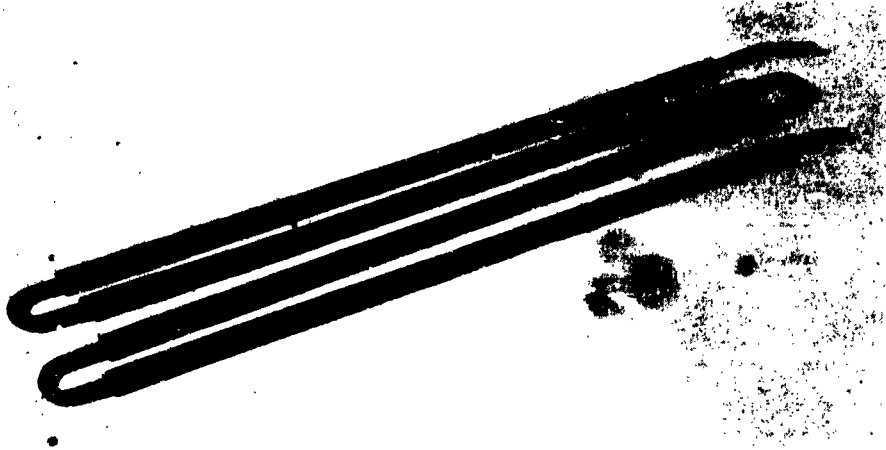
Initial efforts were directed to fabrication of finned tube heat transfer elements representative of the most advanced state of the current art. The heat transfer elements were formed from finned tubing consisting of .005 inch thick stainless steel clad copper fins, 0.375" diameter. Fins were spirally wound, 30 per in., on .188" O.D. stainless steel (type 316L) tubes having a wall thickness of 0.015 inch. The fins were a composite material consisting of 0.0025" copper clad on both sides with 0.00125" stainless steel. A heat transfer element for each heat exchanger is shown in Figure 6.1-1.

Fin material was precoiled and then wound on the tubing into shallow positioning grooves simultaneously formed in the winding process. Subsequent to winding, the finned tubes in straight lengths were sprayed with a nickel base braze alloy to form a thermal bond between the fins and the tube and to protect the exposed copper at the edge of the fin. The turbine heat exchanger tubes were oven brazed in straight lengths and then bent into serpentines. The compressor heat exchanger tubes were bent into serpentines and then formed into involutes before oven brazing. The latter sequence was developed during fabrication of the heat transfer elements and is preferred.

During the production of finned tube serpentines a cracking problem was encountered in several lots of fin material. Tensile tests indicated a ductility of 20% elongation in 6" for this material, which is not sufficient for processing. Additional low temperature annealing treatments produced the required ductility in the fin material. Several rolls of fin material exhibited cladding discontinuities (Figure 6.1-2), but examination of the remainder of the material indicated that this condition was not predominant.

The braze material was sprayed onto the finned tubes before bending. Braze weight was limited to 10% of the finned tube weight. Manual guidance of the spray equipment made control of braze weight difficult and necessitated stripping and re-spraying several tubes with resultant loss in time. Braze weight was controlled on all turbine heat exchanger tubes. However, the press of time required relaxation of braze weight specifications on the compressor heat exchanger tubes. Production quantities would allow mechanical guidance of spray equipment to accurately control braze weight.

HEAT TRANSFER ELEMENTS



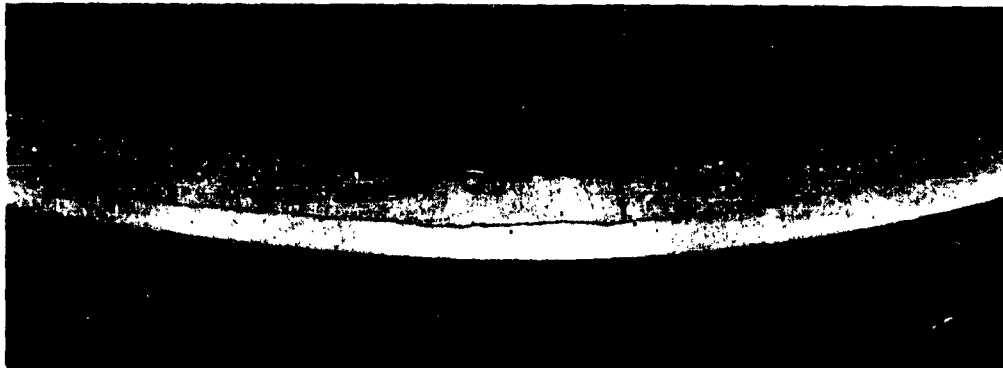
Turbine Heat Exchanger



Compressor Heat Exchanger

5166

Figure 6.1-1



Mag. 100 X

Cross section of fuel material exhibiting a discontinuity
in the protective steel cladding.

4771

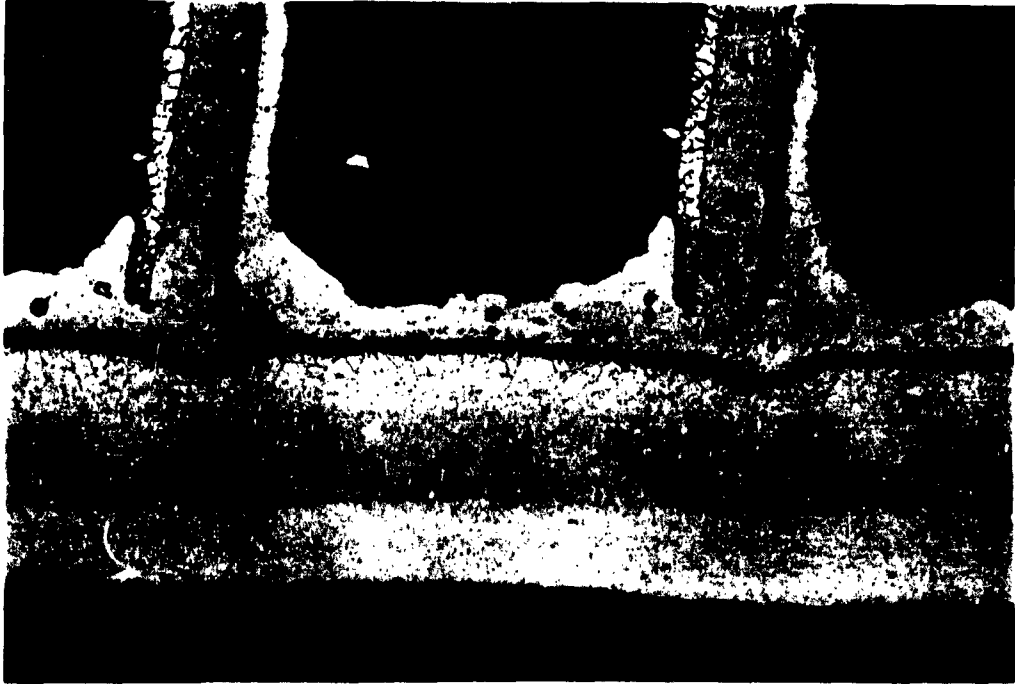
Figure 6.1-2

Turbine exchanger serpentines were oven brazed before bending, necessitating the use of a large vertical retort for brazing. Dew point control is difficult in a retort of this nature, but slight modifications in general practice produced satisfactory samples. Visual inspection of production turbine exchanger serpentines indicated that the overall quality of the elements was marginal and the process control employed would not be sufficient for aircraft quality components. Two elements rejected for mechanical defects, were sectioned and examined metallographically. Figures 6.1-3 and 6.1-4, depict the varying degree of braze quality on these tubes. Poor braze quality resulting in exposure of intermittent areas of copper (Figure 6.1-4) was found, but was not predominant in the sectioned tubes.

The compressor heat exchanger serpentines have an involute configuration which required forming the brazed sections of the tube into a curve. The low ductility of the braze material required that forming take place before the braze was flowed. A new fabrication procedure was developed for these tubes. The braze material was sprayed on with a binder and the tubes were bent and involuted prior to brazing. This allowed the use of a different type of retort and furnace to braze the compressor serpentines. Inspection of completed serpentines indicated good braze flow and coverage.

Tubes for the heat transfer elements were eddy current inspected to a 10% of wall thickness defect level. Finished heat transfer elements were given a 500 psi pressure test followed by helium leak test to a sensitivity level of 1.87×10^{-9} cc of helium per second. All tubes after fabrication were visually inspected under 20X magnification for surface defects.

Prior to fabrication into heat exchangers, the heat transfer elements had support pins torch - brazed to the return bends of the serpentines. The turbine heat exchanger elements had split pins, similar to cotter pins, which wrapped around the tubes. The compressor heat exchanger had split pins butted against the serpentines to avoid interferences during assembly. The nature of the butted pins subjected the serpentines to accidental overheating during brazing. Two defective tubes were found during final leak testing of the compressor heat exchanger. Production quantities of heat transfer elements would have these pins oven brazed under controlled conditions and would eliminate the hazard of overheating.



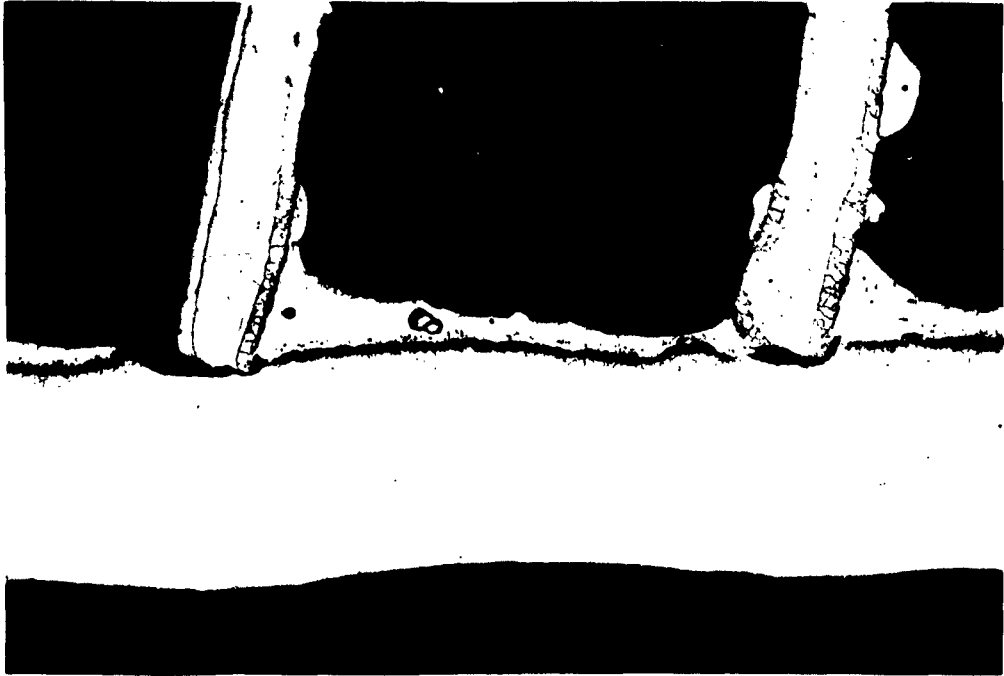
10% HCL Etch

Mag. 100 X

Tube No. 31. Cross-section of finned tube showing good braze flow and coverage.

4785

Figure 6.1-3



10% HCL Etch

Mag. 100 X

Tube No. 117. Cross-section of finned tube showing inadequate braze flow resulting in exposure of intermittent areas of copper.

Figure 6.1-4

6.2 Turbine Heat Exchanger

The turbine heat exchanger was fabricated in two halves with sectioned headers to allow welding of the heat transfer elements from the liquid metal side. The two halves were then joined by welding the header sectors.

Tungsten electrode inert gas welding was used with special techniques to make the tube-to-header welds. The electrode was mechanically driven to generate a circle of compatible size to the tube-to-header welds, Figure 6.2-1. A mixture of helium and argon cover gas was adjusted during welding to establish the arc and maintain optimum gas cover. Welding current was tapered off at the end of the weld to obtain uniform penetration and to avoid thermal cracking. A number of practice welds were made and sectioned to develop reliable procedures. An investigation was made to determine the advisability of trepanning the headers to avoid weld distortion, Figure 6.2-2. Weld distortion was minimized by designing the headers so that welding occurred at the neutral axis. Trepanned welds had no appreciable effect on the small and allowable distortion obtained in test specimens and were eliminated.

Mechanical movement of the electrode allowed rapid welding which minimized expansion strains normally associated with joining light tube sections to heavy-wall headers. Positioning of the tubes under the welding head was done manually and was time consuming. The need for automatic indexing was evident. Automatic indexing was successfully applied during welding of the compressor heat exchanger and appreciably reduced total welding time.

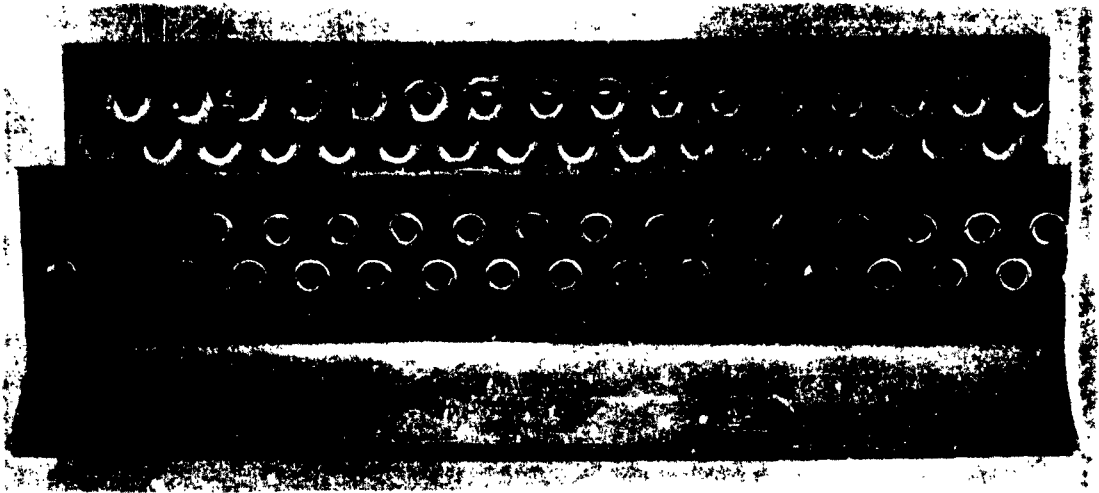
Routine pressure testing of the completed half sections of the turbine heat exchanger, Figure 6.2-3, uncovered a bad leak in one of the tube-to-header welds. An investigation of the tube-to-header welds disclosed large amounts of porosity not previously encountered. Metallurgical studies indicated that oxides were present and that re-welded joints would still be subject to the same porosity. The source of the oxides was attributed to scale on the tubes picked up during brazing of the fins. Stringent mechanical and chemical cleaning procedures were investigated and established. The heat transfer elements were removed from the header sectors by end milling the welds and were subjected to the new cleaning procedures. New headers were made and the tubes rewelded. Limited X-ray examination showed sound welds free from porosity. After making closing welds on the headers the turbine heat exchanger was successfully pressure tested and helium leak tested to a sensitivity of 8×10^{-7} cc of helium per sec.

TURBINE HEAT EXCHANGER
Tube to Header Welding Fixture



Figure 6.2-1

5824

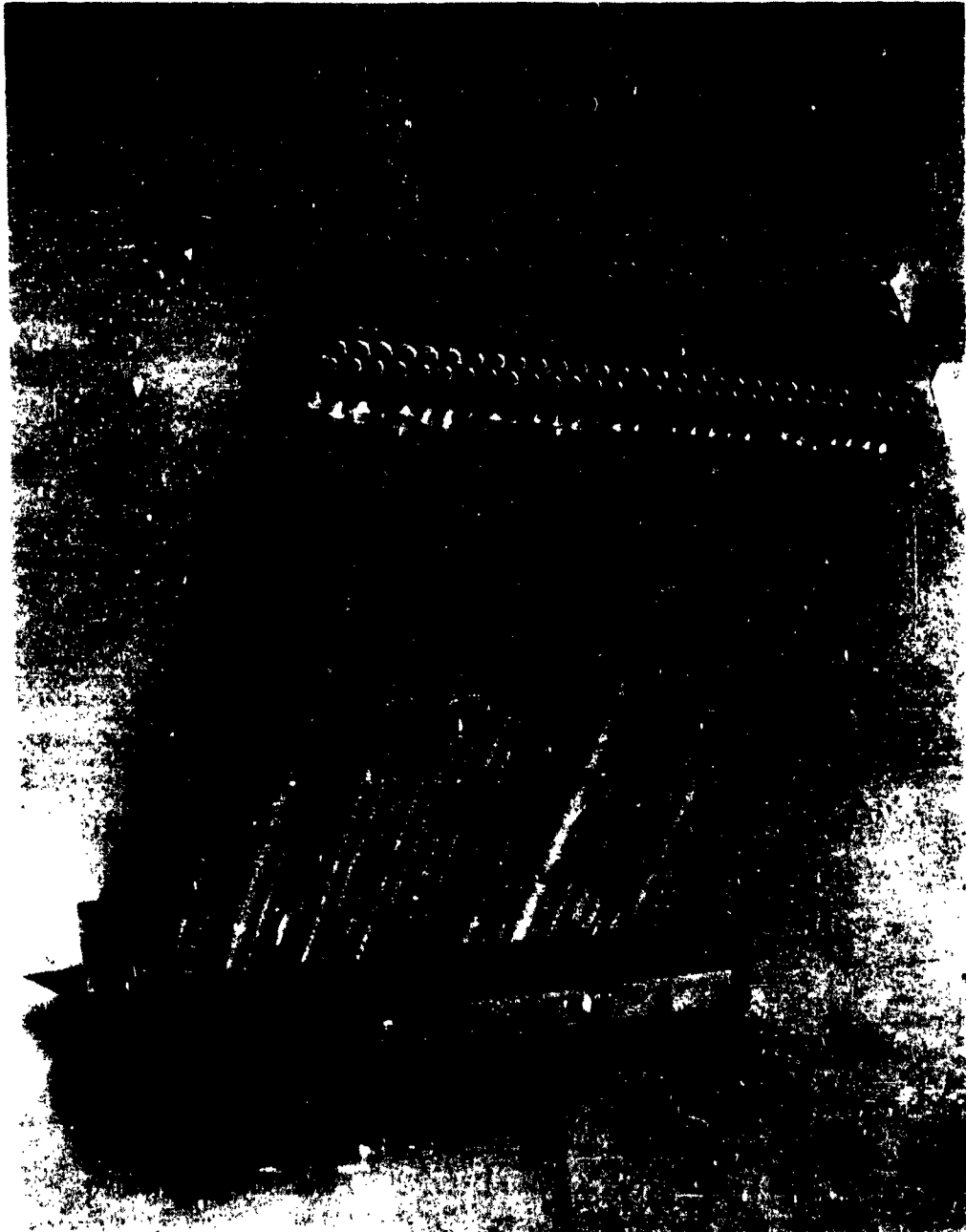


Gross view of sample header sections made with the aid of an ultragraph to evaluate the trepanned vs. the straight (upper sample) tube-to-header joint design.

Figure 6.2-2

4766

TURBINE HEAT EXCHANGER - HALF SECTION



Note: Strap appearing at left hand side is a temporary fixture and is not part of the Heat Exchanger.

5620

Figure 6.2-3

6.3 Compressor Heat Exchanger

The compressor heat exchanger was fabricated after the defective weld experience with the turbine heat exchangers and consequently received immediate benefits of the new cleaning procedures. No welding problems were encountered. However, one tube weld did leak on final pressure test. The header was trepanned to gain access to the weld which was manually rewelded. A gas pocket was detected and eliminated during manual rewelding.

Pressure testing the compressor heat exchanger disclosed two tube leaks in the area of brazed pins. A section at the leaking area of one tube was removed and subjected to metallurgical examination. It was found that the leak was adjacent to a brazed area and that the microstructure (Figure 6.3-1) indicated that the tube had been melted and had absorbed impurities. The two leaking tubes were plugged and welded through access holes obtained by trepanning the headers. Replacement of these tubes would have been a costly and time consuming process. The heat exchanger was then subjected to alternate pressure and helium leak tests to develop and detect dormant leaks that may have resulted from similar mishaps. No leaks developed and the heat exchanger passed helium leak tests to a sensitivity of $8-10^{-7}$ cc of helium per second.

It was postulated that should dormant leaks still be present a short exposure to hot liquid metal would bring them out. A procedure was formulated to detect such leaks during shake-down operation of the liquid metal system. An inert gas smothering system was added to the rig so that any resulting liquid metal fires would be rapidly extinguished and allow salvage of the heat exchanger for repairs.

Three surplus heat transfer elements were installed in a natural circulation liquid metal loop to investigate the development and consequence of dormant leaks. Two of the elements were purposely made defective by drilling holes through the wall and plugging them with braze. A leak developed in one of the plugged holes after two hours of operation at 1200°F and resulted in a liquid metal fire. Burning liquid metal impinged on an adjacent tube and produced another leak. The third tube remained intact. Damage was confined to the area of the leak. It was concluded from this test that defective tubes, if present, would fail during initial operation of the system and that salvage of the heat exchanger was possible.



Fe Cl₃ Etch

Mag. 100 X

Tube bend cross section showing burned area produced
by torch brazing the support pin to the tube.

6.4 Weight of Test Heat Exchanger

The conservative design of the heat exchangers resulted in an increase over the weight target. This weight increase is primarily the sum of many small increments of weight resulting from allowances made for ease of fabrication and assembly and with conservative practical tolerances. Successful fabrication and performance of the heat exchangers indicates that a large portion of the weight increase can be recovered by design refinements. Areas of particular promise are the length of the tangents to the return bends, the length and diameter of support pins, the thickness of the headers at the tube welds, the pin support plates and the baffles.

Closer agreement between the estimated design weight and actual weight was obtained in the turbine heat exchanger than in the compressor heat exchanger. The heat transfer elements of this heat exchanger had the braze weight of the fins controlled to the specified 10%.

Relaxation of the specified 10% braze weight for the heat transfer elements for the compressor heat exchanger, in order to obtain timely delivery, resulted in an increased weight for this heat exchanger. The actual weight exceeded the estimated weight by 33 lbs. Production tooling for braze application could control the braze weight to the 10% specified and probably reduce the braze weight below the specification.

The following weight comparison is based on a complement of two 180° sectors, to form 360° heat exchangers. Comparison is made between targeted, design and actual test heat-exchangers as follows.

	<u>Turbine</u> <u>H.E.</u>	<u>Compressor</u> <u>H.E.</u>	<u>TOTAL</u>
Targeted Weight	130.9	178.6	309
Design Est. Weight	165.6	215.0	380
Measured Weight	161.3	247.8	409.1

A complement of 120° sectors would increase each total weight by approximately 15 pounds. The increase results, primarily, from the necessity of extra, although smaller, headers and extra serpentine return bends and supports. Weight savings considered feasible in the study engine, based on experience gained with the test heat exchangers, are included in Table 5.3-3.

7. TEST EQUIPMENT

7.1 Description of Test Rig

The test rig was primarily designed to obtain state conditions at the heat exchangers as determined by cycle analysis typical of a 3750 HP turboprop engine. The general configuration of the test rig was made similar to the configuration of an engine wherever practical without interfering with the function of the rig. Particular agreement with engine configuration was maintained at the compressor heat exchanger and at the inlet to the turbine heat exchanger. Fig. 7.1-1 shows a section of the test rig and Fig. 7.1-2 shows the completed test rig prior to installation in the test cell.

The large diameter at the outlet end of the rig results from an annular plenum chamber around the turbine heat exchanger which was incorporated to allow the subsequent evaluation of annular diffusers and is not typical of engine configuration. The external structure is included to support the flat end of the plenum against high temperature and pressures incurred in simulating inter-stage conditions of the power turbine.

Although 120° sectors of the compressor heat exchanger and turbine heat exchanger were to be tested, the test rig was made fully circular to allow extended use of the rig for future tests. Internal baffling was provided to confine the air flow to the 120° heat exchanger sectors.

Plant air at 90 psig was supplied to the test rig through a cannular combustor in which unleaded gasoline was burned to elevate the air temperature to simulate compressor discharge conditions. Upon entering the test rig the air was confined to a 120° sector of an annular diffuser which discharged to the 120° axial flow compressor heat exchanger sector. Air leaving the compressor heat exchanger discharged into a plenum containing a single cannular combustor.

The combustor, burning JP5 fuel, elevated the air to turbine discharge temperatures. Immediately after the combustor was a throttle valve to simulate pressure drop through the turbine. Gas leaving the throttle valve encountered a 90° bend and discharged into a plenum chamber to remove velocity head. Exit from the plenum was by means of a series of perforated baffles to induce even distribution of the gases. Downstream of the baffles was a converging section to simulate turbine exit conditions over a 120° annular sector.

The turbine exit sector was followed by a 120° annular diffuser discharging to the radial outward flow turbine heat exchanger. Gas leaving the turbine heat exchanger entered a 120° sector plenum from

TEST RIG

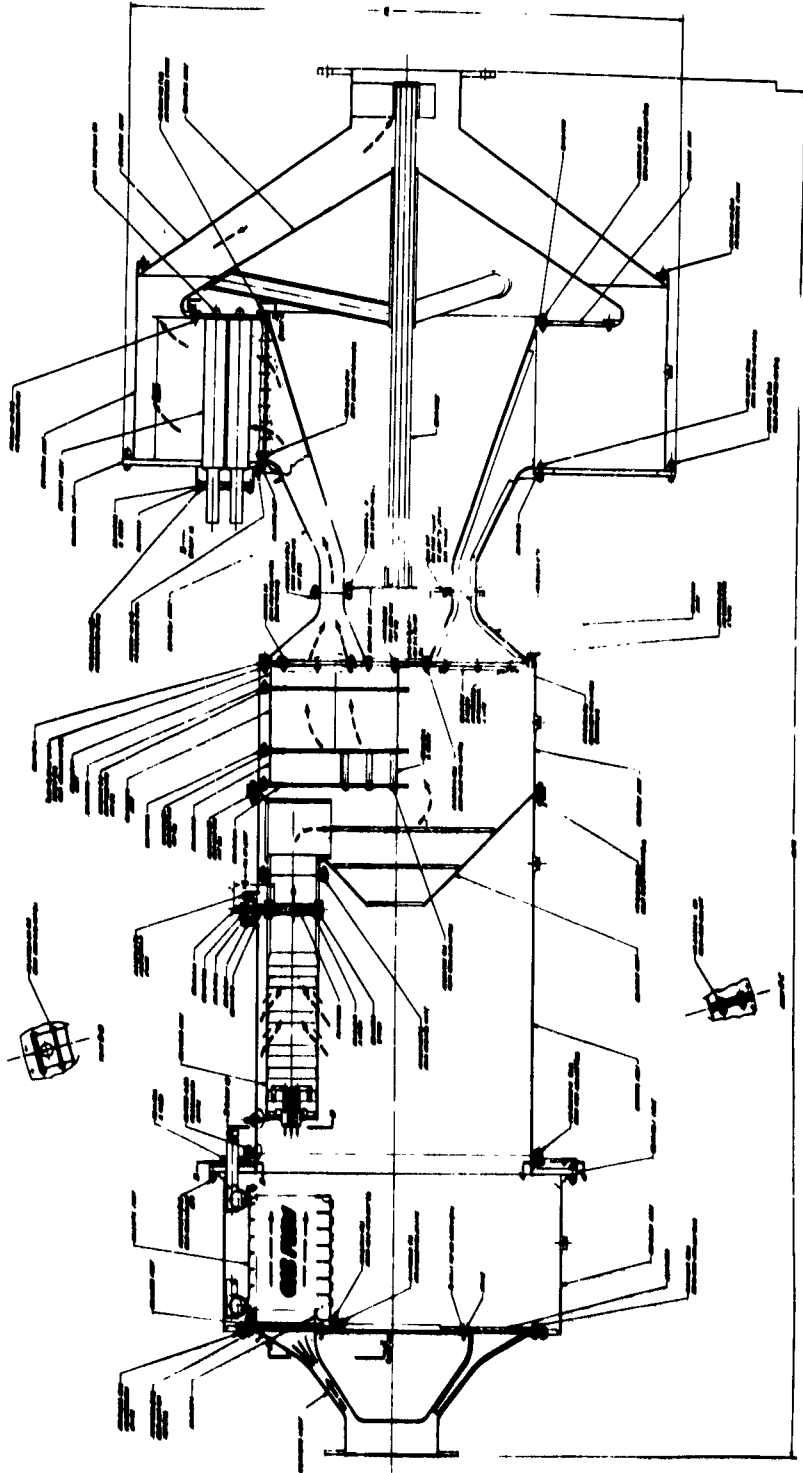
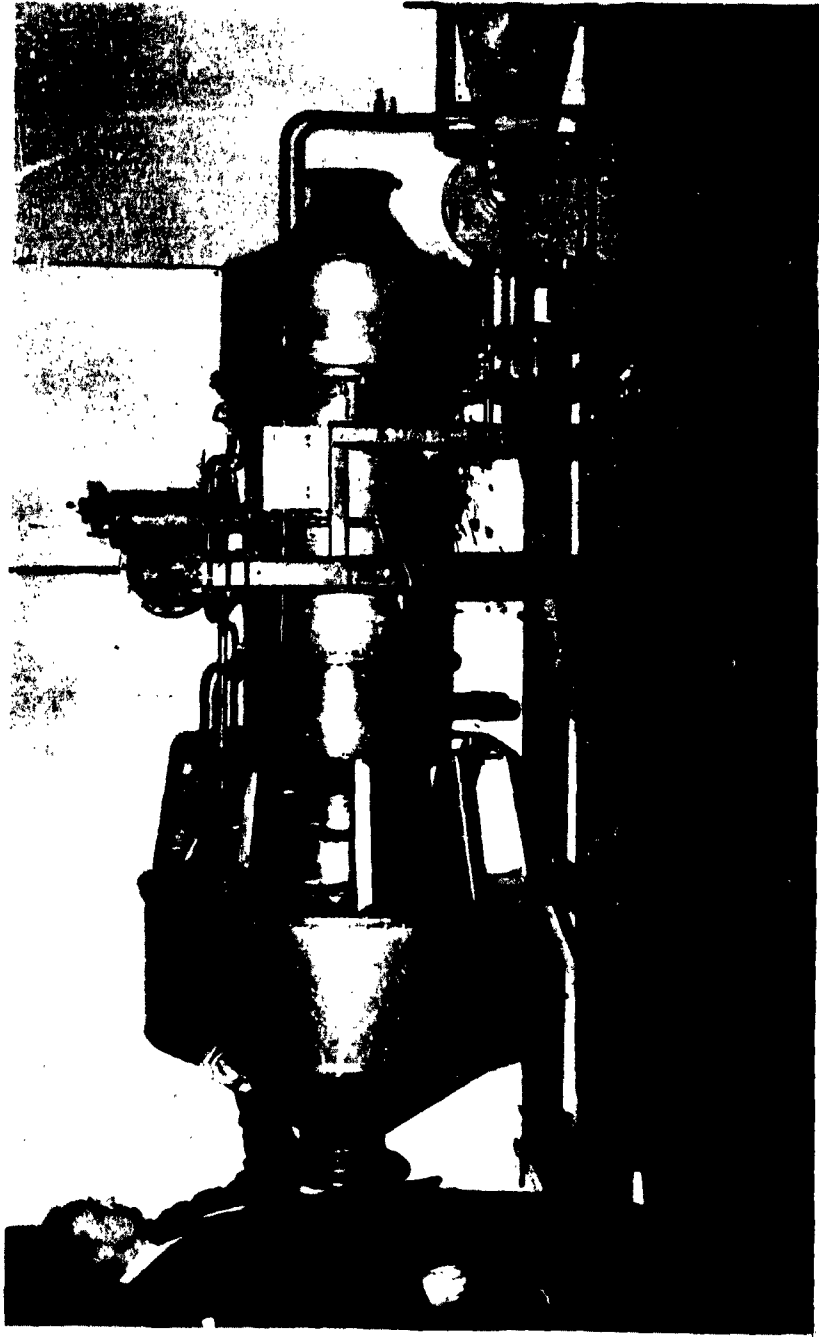


Figure 7.1-1

4702

LIQUID METAL REGENERATOR TEST RIG



5486

Figure 7.1-2

which it was discharged in the aft direction through a conical collector, from which it left the rig through a nozzle. The test rig nozzle discharged at atmospheric conditions into a water spray chamber followed by an exhaust silencer discharging to atmosphere.

Mass air flows and temperatures corresponding to all engine conditions were simulated. Plant air pressure limitations prevented simulation of compressor discharge pressure above engine cruise conditions. Turbine discharge conditions were simulated for all engine loads at sea level conditions. Altitude conditions were not simulated. Aerodynamic loading on the compressor heat exchanger was more severe at high engine loads than would have been encountered in an engine-installation because of the lower air density. The turbine heat exchanger felt full aerodynamic loading at sea level conditions but did not feel aerodynamic loads corresponding to high power levels at altitude.

The design of the diffusers to both heat exchangers was largely experimental because of scant information on large area ratio annular diffusers. The performance of the diffusers was made more difficult to predict because of sectoring and, in the case of the compressor heat exchanger diffuser, the necessity to make the side walls correspond to the involute curves confining the 120° sector compressor heat exchanger. There was concern that the sector diffusers would not behave in the same manner as full annular diffusers and result in uneven distribution of flow over the face of the heat exchangers. Uneven flow distribution over the face of the heat exchangers would seriously impair their effectiveness. Provisions were made for installing screens of various solidity at the discharge of the diffusers to correct mal-distribution of flow should it occur. Recognition of the need to obtain further knowledge on large area ratio annular diffusers was a contributing factor in making a full 360° test rig available for future tests.

7.2 Liquid Metal System

The liquid metal complex consisted of the engine system and the supply system Fig. 7.2-1. The engine system contained the turbine and compressor heat exchangers, connecting lines, pump cell, and expansion tank. This system was complete in itself and is indicative of one of the sector systems forming a complete engine installation. Both heat exchangers of the test system were 120° sectors of full size flight type heat exchangers. The 120° sectors were chosen on the basis of available air supply to simulate engine conditions. The compressor heat exchanger was arranged so that air passed through an annular passage in axial counterflow to the liquid metal, which passed through finned tube serpentine heat transfer elements. The planes of the

LIQUID METAL SYSTEM - SCHEMATIC

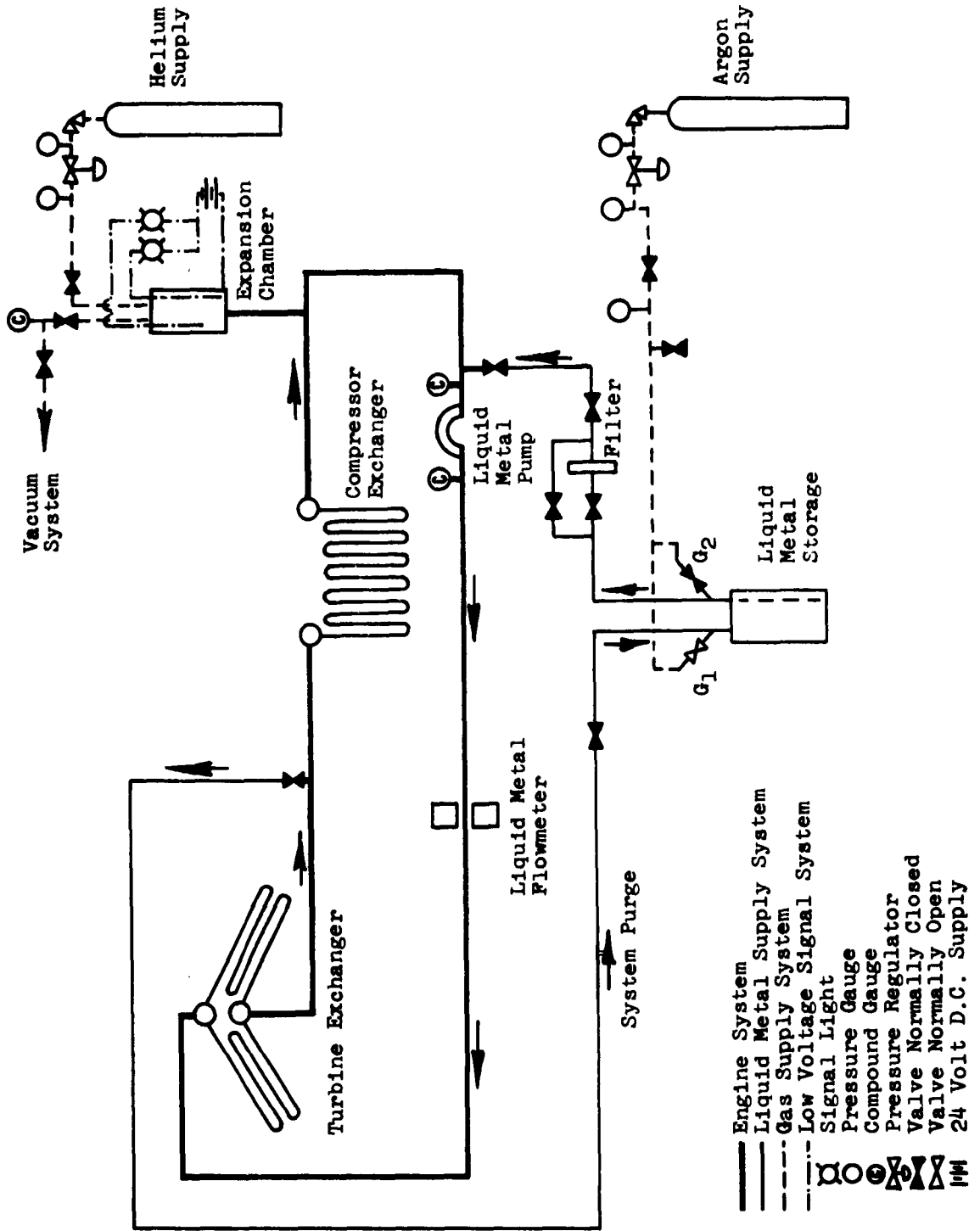


Figure 7.2-1

serpentine were bent to an involute shape to maintain a constant tube spacing throughout the full annular face of the heat exchanger.

The turbine heat exchanger was arranged so that turbine exhaust gases passed radially outward through two bundles of finned tube heat transfer elements connected to centrally located liquid metal headers running fore and aft. Liquid metal passed counterflow to the gas stream. The liquid metal discharged from the turbine heat exchanger directly to the compressor heat exchanger through a pipe line containing an expansion loop which accommodated the relative expansion between the pipe line and the test rig.

The liquid metal discharged from the compressor heat exchanger to a 180° pump cell in which flow of liquid metal was induced by a rotating magnetic field. Liquid metal discharged from the pump cell passed through a liquid metal flow meter to the turbine heat exchanger. The liquid metal flow meter was for test purposes only and is not required in a flight system. The flow meter was an electromagnetic device in which a voltage, indicative of the flow, was induced by the liquid metal flowing through a magnetic field. The flow meter required long runs of straight pipe fore and aft, to establish normal turbulence similar to the requirements of an orifice type flow meter. The introduction of the flow meter into the system greatly extended the length and complexity of piping.

An expansion tank was included in the system to accommodate the expansion of liquid metal from cold start conditions to operating temperatures, and was connected to the suction side of the pump for ease of maintaining and monitoring pump suction conditions. The expansion tank contained helium as a cover gas to maintain system pressure. High level and low level probes, which completed low voltage circuits when in contact with liquid metal, were utilized to monitor the amount of liquid metal in the system. The size and complexity of the expansion tank were determined by test requirements and are not indicative of flight type expansion tanks which can be made more compact.

The supply system in support of the engine system included a liquid metal supply tank, a liquid metal supply line from the supply tank, a liquid metal filter and a liquid metal return line to the supply tank. Included in this system were liquid metal supply and return valves, inert gas pressurizing lines, and a vacuum system. The function of the auxiliary system was to load and purge the test system and is indicative of a service facility and not of flight hardware.

7.3 Liquid Metal Pump

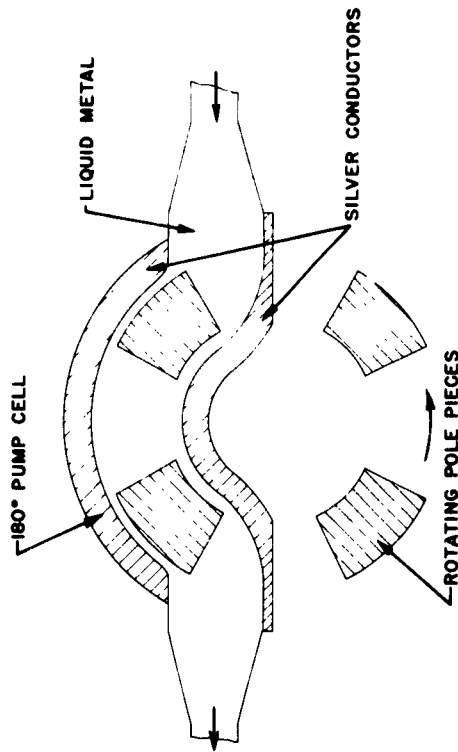
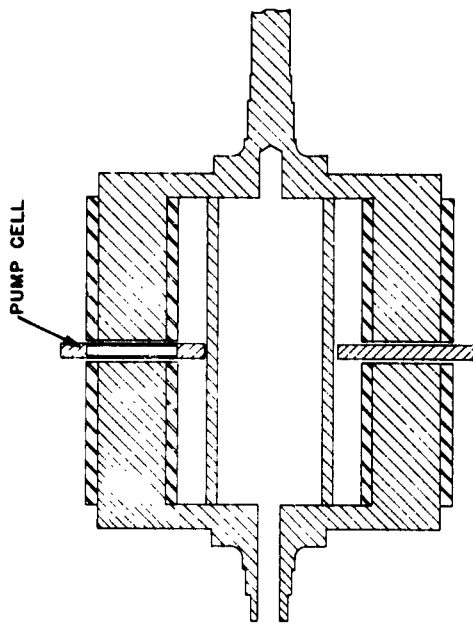
Liquid metal was circulated by means of a special electrodynamic pump Fig. 7.3-1. The pump consisted of a magnetic rotor which swept over a fixed pump cell made integral with the liquid metal system Fig. 7.3-2. The rotor contained permanent magnets in axial alignment near its periphery with an axial air gap at the middle of the rotor. The pump cell, in the form of a flat 180° annular sector, was so positioned in the air gap that the pole faces of the magnets repeatedly swept the circumferential length of the cell.

The magnetic fields bridging the air gap passed through the conducting liquid metal and induced eddy currents in the liquid metal. The eddy currents in turn created magnetic fields opposing the magnetic field of the rotor and displaced the liquid metal by magnetic repulsion. The cumulative effects of the eddy current action produced a continuous flow of liquid metal through the pump cell.

The pump cell contained silver conductors at the inner and outer peripheries which provided return paths for the heavy eddy currents induced in the liquid metal. In this manner heavy electrical currents necessary for electromagnetic induction were produced and confined within the pump cell and no external electrical source was required.

The flat configuration of the pump cell required the use of pin reinforcements which axially spanned the passage area. These pins generated high internal hydraulic friction and limited the capacity of the pump. A re-evaluation of the pump cell design showed that a construction using concentric elliptical liquid metal passages was feasible and would reduce the internal pressure losses. A pump cell was made using this construction. Hydraulic tests have shown a 50% reduction in internal losses. Actual pumping tests have not been run because the inclusion of the new pump cell would have required an extensive rework of the liquid metal system in a prohibitively short time. This pump is a variation of commercially available electrodynamic pumps in which the magnetic field is produced by electromagnets acting on a full 360° pump cell. The object of the pump procured was to demonstrate the feasibility of using 2 or more independent pump cells each integral with separate liquid metal systems and to demonstrate the feasibility of using permanent magnets in lieu of electromagnets. Cost and time permitted only a demonstration of principles of operation applicable to the design of a flight weight pump. No attempt was made to refine the pump and achieve flight weight construction.

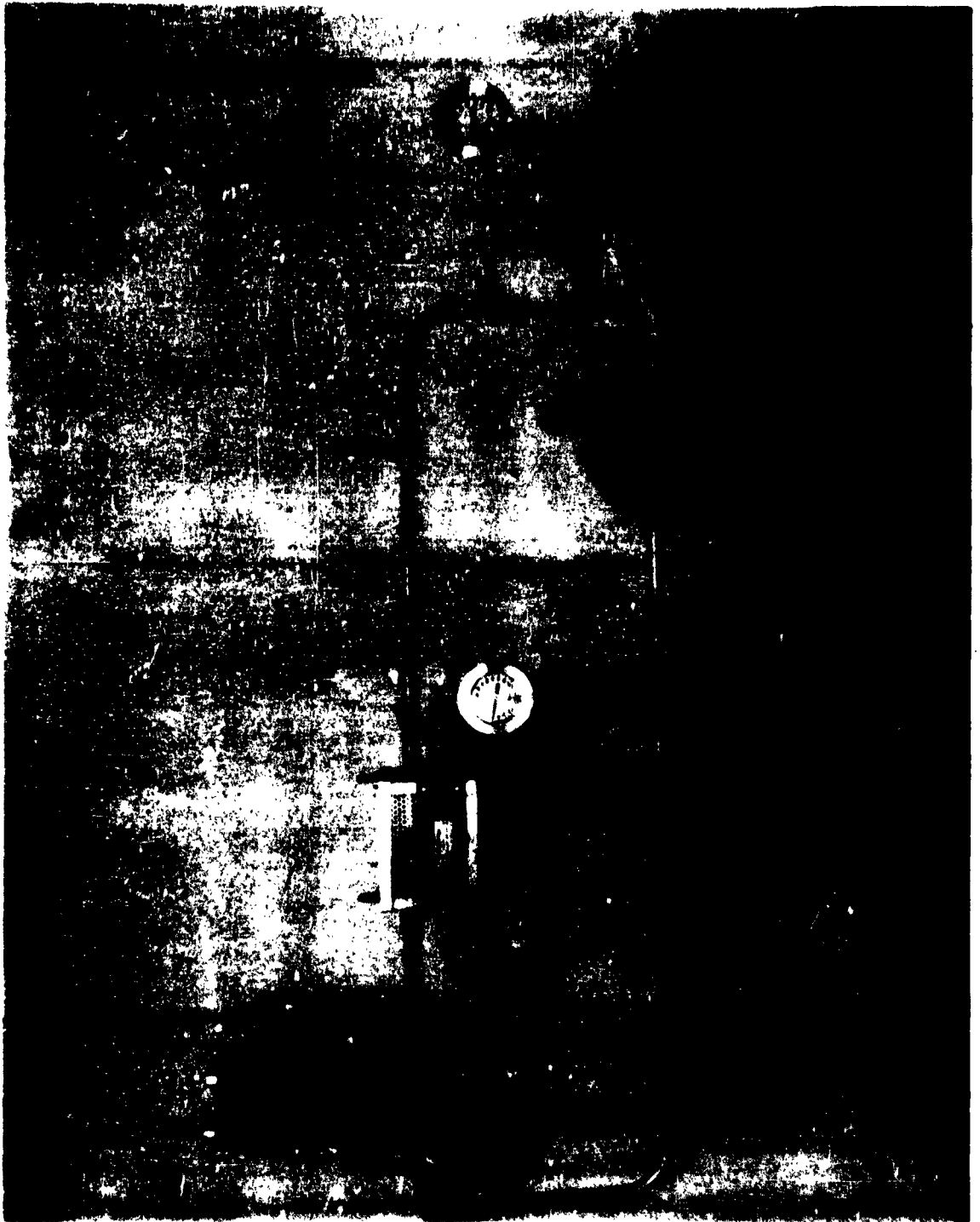
LIQUID METAL PUMP



4770

Figure 7.3-1

LIQUID METAL PUMP - TEST LOOP



5819

Figure 7.3-2

7.4 Instrumentation

Pressure and temperature probes were located at both faces of the two heat exchangers to determine performance within each heat exchanger. Total pressure probes were used to determine pressure distribution across and through each heat exchanger.

Continuity of performance between the turbine heat exchanger and the compressor heat exchanger was monitored by the temperature of the circulating liquid metal before and after each heat exchanger. Liquid metal system performance was sensed by surface thermocouples welded to the circulating lines, a liquid metal flow meter, and bourdon tube pressure gauges located in the pump suction and discharge.

The liquid metal heat exchangers were monitored for leaks by bleeding gas from the test rig after each heat exchanger and passing this gas continuously through a bunsen burner flame. A leak would have been detected by the pronounced yellow flame caused by minute amounts of sodium. Further monitoring of the liquid metal system was accomplished by the low level probe and a pressure gauge located at the expansion tank.

All air and gas side instrumentation was conventional. A tabulation of this instrumentation and the liquid metal instrumentation appears in Figure 7.4-1.

Instrumentation List

<u>Air Side</u>	<u>Flow</u>	<u>INSTRUMENT PROBES</u>		<u>Level</u>
		<u>Pressure</u>	<u>Temp.</u>	
Air Supply	1	2	2	
Preheater Fuel	1	1	1	
Preheater			1	
Inlet Diffuser Exit Face		2	3	
Comp. Heat Exchanger-Inlet Face		7	2	
Comp. Heat Exchanger-Outlet Face		4	8	
Combustor Fuel	1	1	1	
Combustor and Discharge Plenum		3	2	
Turbine Heat Exchanger-Diffuser		2	3	
Turbine Heat Exchanger-Inlet Face		18	3	
Turbine Heat Exchanger-Outlet Face		4	12	
Turbine Heat Exchanger-Collector		$\frac{3}{47}$	$\frac{4}{42}$	
<u>Liquid Metal Side</u>				
Pump	1	2	3	
Compressor Heat Exchanger-In			1	
Compressor Heat Exchanger-Out			1	
Turbine Heat Exchanger-In			1	
Turbine Heat Exchanger-Out			1	
Expansion Tank	$\frac{4}{4}$	$\frac{1}{50}$	$\frac{49}{49}$	$\frac{2}{2}$

Miscellaneous instrumentation included means of measuring liquid metal pump speed and power input.

Figure 7.4-1

7.5 Cold Start Rig

The behavior of liquid metals under cold start conditions was investigated by a simple apparatus (Figure 7.5-1) which simulated the effects of the various components of a liquid metal regenerator system. A single finned tube serpentine heat transfer element was welded on both ends to a common header which in turn was connected to a small expansion tank by a tube representative of the liquid metal circulating lines of a liquid metal regenerator system. Since the object of the test apparatus was to investigate only the pressure-relieving capacities of chilled liquid metal there was no need to provide for circulation of the liquid metal.

Provisions were made to immerse the test apparatus into a cold box capable of reaching -65°F . The exhaust duct of a 60 HP gas turbine was modified to receive the chilled apparatus and to expose the finned tube serpentine directly to the turbine exhaust at start-up conditions. Test conditions were made unusually severe by allowing direct impingement of high velocity exhaust gases on the finned tube serpentine. Test conditions were purposely made severe to determine the extent of problem areas if these existed.

TEST APPARATUS FOR COLD START INVESTIGATIONS



Figure 7.5-1

8487

8. TEST PROGRAM

8.1 Rig Tests

Prior to installation of the liquid metal regenerator system, the test rig was operated over the full range of simulated engine conditions. Observed data indicated reasonably good gas distribution downstream of the diffusers leading to the compressor and turbine heat exchangers.

Testing of the liquid metal regenerator system was preceded by loading liquid metal to the system and by a short shakedown operation to prove out the integrity of the system. Preloading operations consisted of several evacuations and helium fills to purge oxygen from the system. This purging was followed by a short run at elevated temperatures to remove adsorbed oxygen and to evaluate the integrity of the system under thermal stress conditions. During loading of liquid metal the rig pre-heater was fired to maintain rig temperature at 300°F to accelerate liquid metal flow. Liquid metal was displaced from a sealed storage tank into the evacuated system by pressurizing the tank with argon.

Initial operation of the system was conducted to develop dormant leaks by the action of hot liquid metal. System temperature was maintained at 600°F by the rig pre-heater and liquid metal was circulated. The system was monitored for leaks by bleeding gas from the rig downstream of each heat exchanger. The bled gas was passed through a bunsen burner flame in search of the telltale yellow flame of sodium.

Following initial operation, the system was purged to remove dissolved oxides. Operation was the same as initial operation except loading and venting valves were opened to allow by-pass circulation between the system and the storage tank. By-pass circulation was maintained by adjusting system pressure, pump suction pressure, and storage tank pressure. The system content was monitored by high and low level probes in the system expansion tank. The storage tank was cooled with air to promote precipitation of oxides on the tank walls. Liquid metal flow from the storage tank to the system was through a filter to remove any suspended oxides. Upon completion of the purging operation, the system was ready for exchanger-evaluation tests.

Initial testing was performed by simulating various engine conditions. Analysis of data showed uneven temperature readings before and after the compressor heat exchanger. This behavior was attributed to uneven temperature and gas distribution to the heat exchanger. In order to obtain reliable inlet temperature conditions, a series of tests were

run with cold air entering the compressor heat exchanger. This mode of operation greatly increased temperature differentials throughout the regenerator system. However, the floating support system of the heat transfer elements allowed safe operation at these conditions.

Analysis of data now clearly showed uneven gas distribution in both heat exchangers and a resulting fall-off in effectiveness. High solidity screens were placed before each heat exchanger in efforts to improve distribution. No appreciable benefit was obtained. It became evident that a major rework of the test rig was needed to improve gas flow distribution to the heat exchangers.

During installation of the screens, both faces of the heat exchangers were observed for soot build-up and were found free of fouling except for the trailing edge of the last row of tubes in the turbine heat exchanger. This examination took place after 40 hours of operation.

Insufficient time remained to both rework the test rig and to accumulate sufficient operating hours to evaluate durability. Believing that evaluation of durability was paramount, a decision was made to forego improving the performance of the test rig. Efforts were directed towards obtaining maximum operating hours on the system.

Runs were made to simulate various engine loads to 70 percent power at sea level conditions. This range of power levels included maximum predicted turbine exhaust temperatures. An arbitrary line was drawn at this power level as it was felt that uneven gas distribution and the resulting steep temperature gradients could already be taxing the system beyond take-off conditions. Although confidence in the system was high, it seemed unwise to jeopardize more profitable endurance running by chancing unmeasurably severe operating conditions.

A program of continuous running at cruise conditions was initiated to evaluate fouling. This run lasted 41 hours before a shutdown was forced by erratic burner behavior. A two hour interruption of running time occurred because of troubles with the fuel supply to the pre-heater. After 20 hours of operation the exhaust became smokey. As burner performance deteriorated, evidence of fouling, though small, became more pronounced. A decision was made to keep running as operation with poor combustion would be relevant to emergency engine operation.

About midway in the test program, a fire occurred in the test rig as the result of a faulty fuel valve. After the prior routine shutdown, fuel leaked through this valve and drained from the cooled combustor into the still hot test rig and ignited. This fire remained undetected until the magnitude was great enough for smoke accumulations to be

noticed. The fire was extinguished by flooding the rig with argon.

The nature of the smoke and observation of system pressures indicated that the fire was not of liquid metal origin. Opening of rig vent valves showed raw fuel accumulations and led to the detection of the faulty fuel valve. After correcting the fuel valve and blowing the system clear of fumes, testing was continued.

Continuation of testing was based on the assurance that the heat capacity of the liquid metal system protected the heat exchangers from overheating. Subsequent examination of the heat exchangers was made shortly thereafter, during a partial disassembly of the rig to install screens for improvement of diffuser performance. The examination showed that the fire had produced no damaging effects.

8.2 Liquid Metal Thermal Convection Loops

To obtain advance knowledge of materials compatibility and mass transfer effects, two liquid metal (NaK) loops were fabricated and tested. The loops were designated Loop A and Loop B and were set up in such a manner as to study the effects of mass transfer on thin walled tubes at the hot exchanger and clogging as a result of mass transfer at the cold exchanger test unit (see Figure 8.2-1). No extreme measures were taken to remove the oxides from the liquid metal prior to charging the system.

The configuration of Loop A consisted of two 8 inch long single pass heat exchangers having 19 stainless steel type 304, 0.020 inch wall, .185 inch O.D. diameter tubes welded in a circular tube bundle 1-7/16" diameter. The loop was operated at 1100°F at the hot end and approximately 500°F at the cooler end.

After 300 hours of endurance, clogging was noted in the cold exchanger. An investigation of the loop showed that leaks had developed in the loop test equipment system (not the test specimens) and oxide impurities which entered the system resulted in clogging the cold exchanger. During this investigation the heat exchanger test units were cut out from the loop and inspected. No perceptible evidence of mass transfer of the tube material was noted. The test sections were reinstalled in the loop and endurance testing continued. Operation was normal and continued for a total of 3024 hours. At this time the loop was dismantled and inspected. There was no evidence of mass transfer, deterioration, or plugging. See Figures 8.2-2 and 8.2-3.

LIQUID METAL CONVECTION LOOPS FOR MATERIALS COMPATIBILITY STUDY

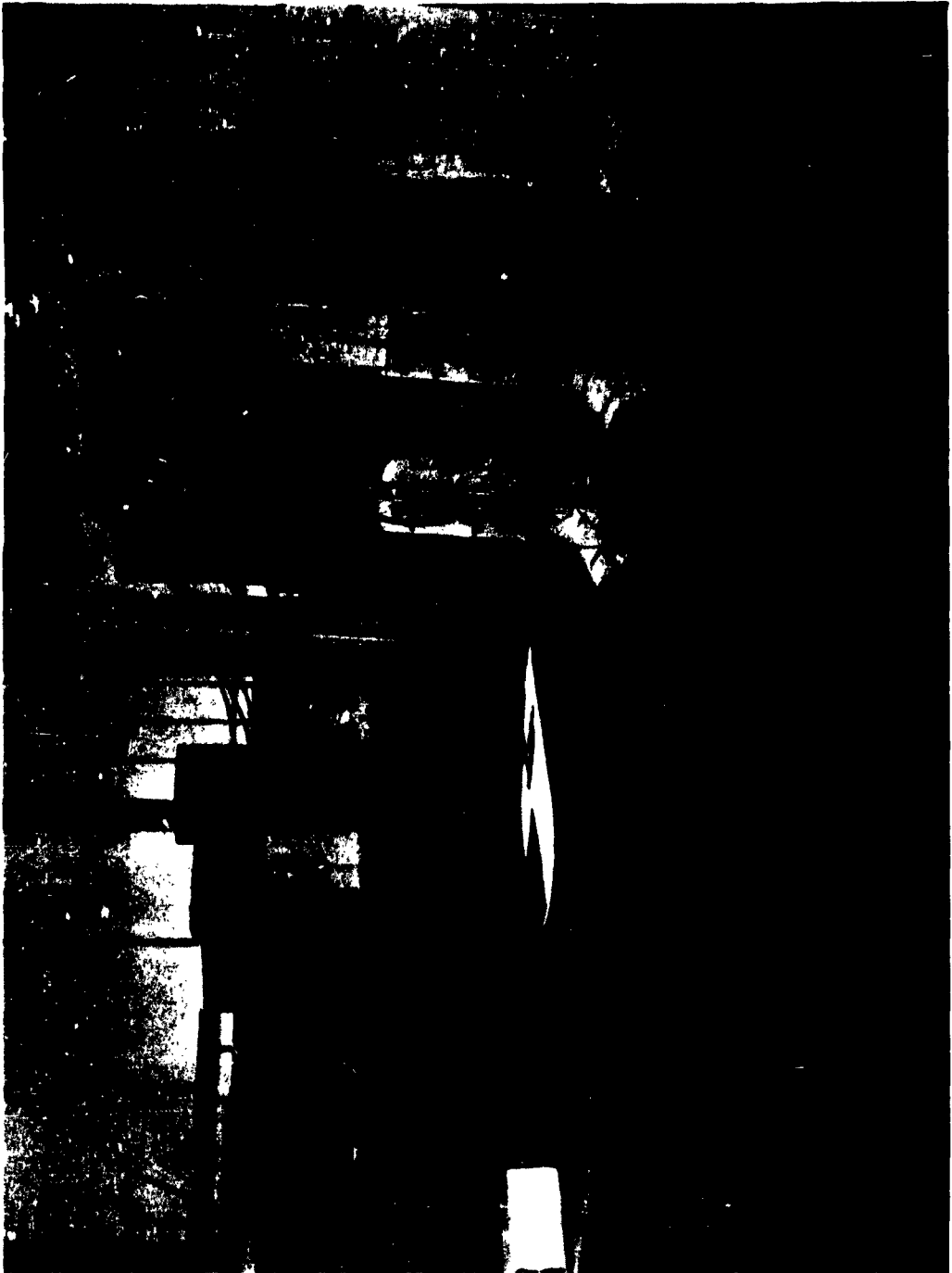


Figure 8.2-1

5295

LIQUID METAL LOOP HEAT EXCHANGER
After 3024 Hours of Operation



Figure 8.2-2

5621

**LIQUID METAL LOOP HEAT EXCHANGER
Heads and Tube Sheet After 3024 Hours of Operation**



Figure 8.2-3

5435

Loop B incorporated similar test heat exchangers and test conditions as those evaluated in Loop A. The tube elements of the heat exchangers were made of .016" wall tubing. Circulation rates, deduced by heat and wattage balances, in this loop were 8 ft. per min. in the heat exchanger tubes and 12 ft. per min. in the connecting tubes. These low flow rates made the loops sensitive to plugging. After 2736 hours of operation some evidence of plugging in the loop was indicated by an increase in temperature differential between the hot and cold legs. The plugging condition was relieved by reducing the cooling air supply to the cold legs of the loop for approximately two days. Normal operating temperatures were restored and loop operation continued at rated capacity. A gradual plugging was again noted after 3456 hours of operation. The same procedure to alleviate this condition was applied and the loop returned to normal operating conditions. Satisfactory operation continued for an additional 366 hours. At the end of this period, the loop again started plugging. After an additional 192 hours, during which time plugging became more severe, operation was discontinued. Total operating time at shutdown was 3982 hours. The loop was dismantled and an investigation made of the conditions of the test heat exchangers. Chemical and metallographic analysis revealed that plugging was primarily caused by contamination of the NaK with silicon during a previous test with glass elements and was not due to corrosion or mass transfer effects. Primary plugging occurred in the area of a dead-ended "Tee" which acted as a trap and collected impurities. The heat exchanger elements were in excellent condition, with minimum deposits, and free from plugging.

8.3 Low Temperature Liquid Metal Alloys

A small investigation was carried out to determine the behavior of Cesium NaK alloys at -65°F . Increment amounts of cesium were added to high potassium NaK alloys. Cooling curves were obtained and thermal arrest points determined. Data obtained allowed a binary curve of cesium and NaK 77 (77% potassium) to be plotted. From this curve it was deduced that an alloy containing 56-58% cesium would be 100% liquid at -65°F . The amount of alloy liquid at -65°F for lower cesium content was also determined from this curve.

On the hypothesis that a 100% liquid state would not be required for successful cold starts of a liquid metal regenerator system a 10% cesium NaK alloy was subjected to screening tests. NaK 56 (56% potassium) was also subjected to the same tests to obtain a reference. Test apparatus containing surplus heat transfer elements from a previous program was constructed to simulate the principal components of a liquid metal regenerator system. Separate apparatus, respectively containing 10% cesium NaK and NaK 56 were precooled to 50°F -15°F and -65°F and were subjected at these temperatures to the exhaust of a 60 HP gas turbine during start up.

The operating conditions were more severe than expected service conditions in that high velocity exhaust gas impinged on only a portion of the chilled heat transfer element. This mode of operation produced abnormally high heating rates on portions of the heat transfer elements while other portions remained virtually cold.

9. RESULTS & DISCUSSION

9.1 General

High performance flight weight liquid metal heat exchangers have been made and tested. Compatibility with efficient engine configuration has been demonstrated as well as durability in engine environments. Fabrication of these heat exchangers required the development of light weight, high performance, finned tube heat transfer elements. Procedure developed in the fabrication of these heat transfer elements provide a firmly established advance in the art of manufacturing high temperature finned tube elements for liquid metal service.

A prototype of an advanced concept in liquid metal pumps has been made and has successfully demonstrated principles of operation essential to application of liquid metal regeneration to aircraft engines. Adequate circulation of liquid metal in the sealed sector of the regenerator system has been effected by rotating permanent magnets. Flow is induced magneto-hydrodynamically in the pump cell which is integral with the system. The cell is mechanically independent of the rotating elements of the pump. Verification has been obtained of the practicability of installing the liquid metal regenerator system in self-contained sealed sectors.

9.2 Durability

The total operating time of the liquid metal regenerator system in the test rig was 116 hours. Of this operating time, 97 hours was run with the liquid metal at elevated temperatures. The difference of 19 hours included operation of the system at elevated temperatures without liquid metal and operation with liquid metal at cold conditions. Operation at various engine conditions amounted to 58 hours. The remaining hours were run to obtain basic performance data. The majority of these hours was at operating conditions more severe than engine conditions in that the liquid metal system was subjected to temperature differentials greater than anticipated for normal operation.

Engine conditions were simulated up to 70% power at sea level and included the maximum predicted operating temperature of 1200°F. Attainment of higher load conditions was not attempted because of lack of opportunity to correct the test rig to obtain even distribution of gas to the heat exchangers. There was concern that pressure loadings and steep temperature gradients caused by uneven distribution of gas had produced operating conditions of severity equal to, if not greater than, take-off conditions.

A total of 20 starts were made which required the light-off of both combustors. Combustors were lit separately and on occasion the preheater

Hours	Corrected Air Flow LBS/HR	GAS SIDE				Press Range PSIG
		Pressure Range PSIG	COMPRESSOR HEAT EXCHANGER		Range	
			Temp. Inlet °F	Temp. Outlet °F		
10:10	11,000	12.7-55	83-420	515-750	.6-1.	
	TO					
9:45	12,000	63-77	95-535	330-820	.9-1.	
	TO					
:40	13,000	68-69	440-455	705-755	1.2-1.	
	TO					
52:40	14,000	18-83	77-550	420-770	.9-1.	
	TO					
1:45	15,000	83-84	530-540	780-840	1.6-1.	
	TO					
7:00	16,000	23-85	85-555	365-735	1.2-2.	
	TO					
2:00	17,000	68-83	85-580	530-925	1.6-2.	
	TO					
:20	18,000	81-81	92-95	645-685	1.9-2.	
	TO					
	19,000					
13:25		Miscellaneous Operation - Zero NAK Flow With Hot NAK Adjust Operati				
<u>97:45</u>		Total Operating Time With Hot Liquid Meta				
13:55		Miscellaneous Operation - Pump Tests - Co With Cold NAK				
<u>111:40</u>		Total Operating Time With Liquid Metal In				
5:05		Miscellaneous Operation - Cold Flow Test Heat Exchangers Without Liquid Metal, Out				
<u>116:45</u>		Total Rig Time With Heat Exchangers				



SUMMARY OF OPERATING CONDITIONS

GAS SIDE		LIQUID METAL			Power Level Corresponding To Air Flow & Remarks
TEMPERATURE RANGE		Pressure	Temp	Flow	
Inlet °F	Outlet °F	Range PSIG	Range °F	Range GPM	
500-1050	310-700	15-51	113-872	0-34.2	20% NRP SLS
660-1050	480-785	13-53	225-850	20-30	60% NRP - 15,000 FT-240 KN Initial Operation & Purge
960-998	690-730	25-52	550-810	333-333	30% NRP SLS
540-1020	475-735	14-53	101-895	0 -34.7	35% NRP - 1500 FT-225 KN
1040-1050	760-800	23-52	575-950	20-30	40% NRP - SLS
575-1150	385-790	15-54	100-1055	0 -34.2	50% NRP - SLS
770-1200	485-900	15-57	300-1020	34-35	70% NRP - SLS (Max. Temp) 75% NRP - 10,000 FT-350 KN
995-1010	475-570	17-43	280-785	30-30	75% NRP - SLS

Start Up - Shut Down
Points - Rig Checks - Loading

Air Tests Up To 21,500 LB/HR

stem

To 21,700 LB/HR
sing up to 1135°F

TABLE 9.2-1



combustor was shut off after light-off to run certain performance tests. The liquid circulation rate was varied throughout all tests and on occasion was reduced to zero. A summary of the test conditions is given in Table 9.2-1.

9.3 Performance

Performance evaluation of the liquid metal regenerator system was based on a special series of tests selected to keep system variables to a minimum. Liquid metal flow was varied from maximum to zero for three different air flows and the effects noted by temperature readings throughout the system. A summary of the data from these tests is plotted in Figure 9.3-1.

Tests were conducted with unheated inlet air to the test rig in order to obtain uniform temperature distribution to the compressor heat exchanger. Even temperature distribution to the turbine heat exchanger was assured by a mixing chamber in the test rig between the combustor and this heat exchanger. The fuel-air ratio of the main combustor, which simulated turbine discharge temperature, was kept constant for each air flow. In this manner the variations in system temperatures were responsive only to the degree of regeneration as determined by the flow of liquid metal. The initial set-point for each series of runs was arbitrarily selected as 1000°F inlet temperature to the turbine heat exchanger when liquid metal flow was maximum.

Overall effectiveness of the system was determined both from the heat gained by the air passing through the compressor heat exchanger and from the heat lost by the gas passing through the turbine heat exchanger. These overall effectivenesses are compared to predicted overall effectivenesses for each air flow in Figures 9.3-2 to 9.3-4. The predicted effectivenesses for the test conditions are lower than the effectivenesses for engine conditions because lower air temperatures to the heat exchangers depresses the gas side heat transfer rates.

Effectiveness is plotted against corrected liquid metal flows which were calculated from the heat capacity of the gases and the liquid metal temperatures for each case. Liquid metal flow was deduced, since the liquid metal flow meter appeared to be off calibration. Discrepancies between the two performance curves is attributed to experimental error introduced by insufficient instrumentation to fully measure the effects of mal-distribution of gases to the heat exchangers. Temperature gradients downstream of both heat exchangers indicates uneven distribution of flow through the heat exchangers. Uneven distribution is primarily attributed to the performance of the sectored, large area-ratio diffusers upstream of each heat exchanger. Uneven distribution is also attributed to bypassing of air within the heat exchangers.

SYSTEM TEMPERATURES vs NaK FLOW

- 762 lbs/hr JP5 - 11,350 lbs/hr Air
- 924 lbs/hr JP5 - 14,200 lbs/hr Air
- △--△ 1080 lbs/hr JP5 - 16,400 lbs/hr Air

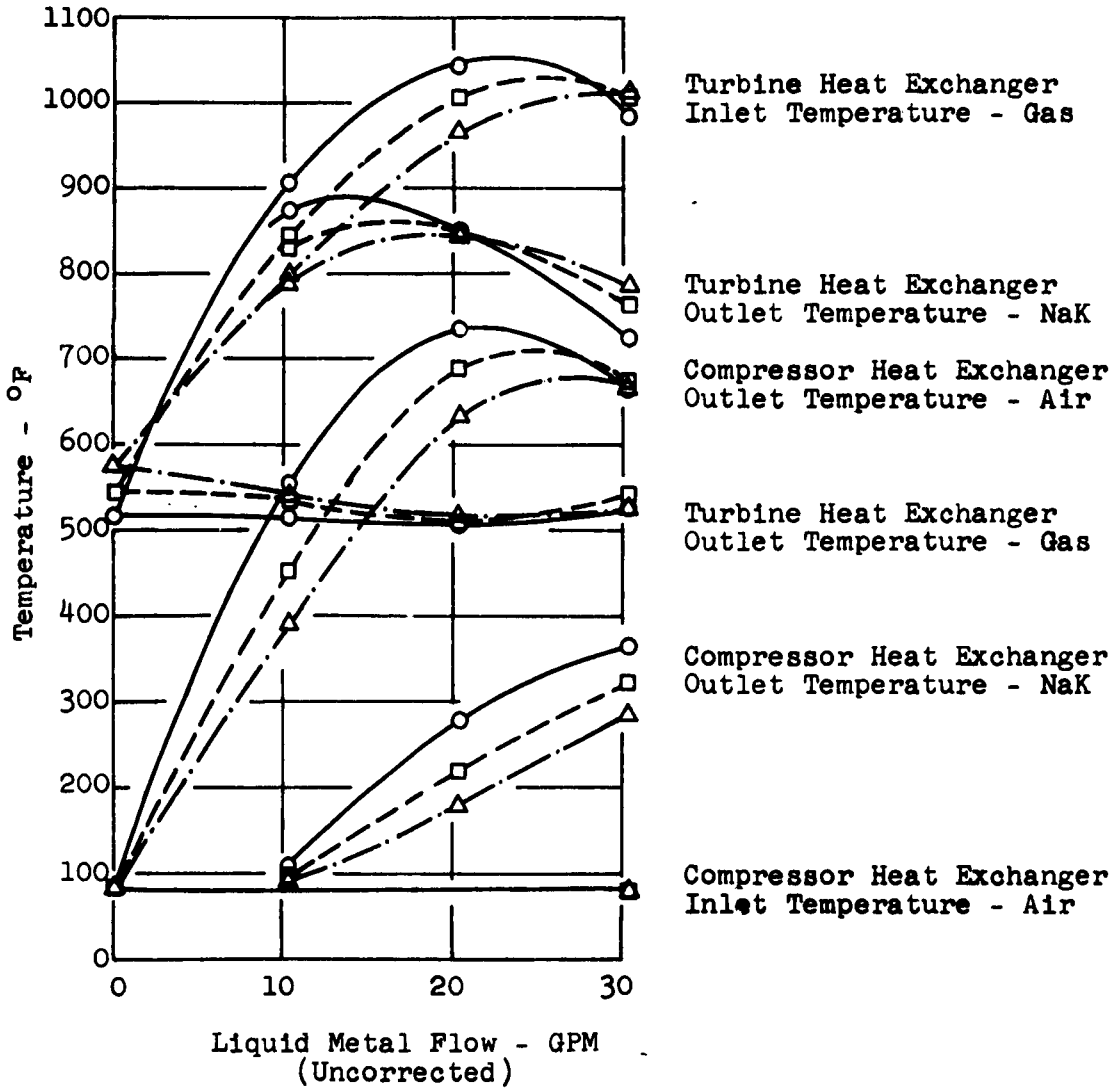


Figure 9.3-1

5897

OVERALL EFFECTIVENESS
vs
CORRECTED NaK FLOW

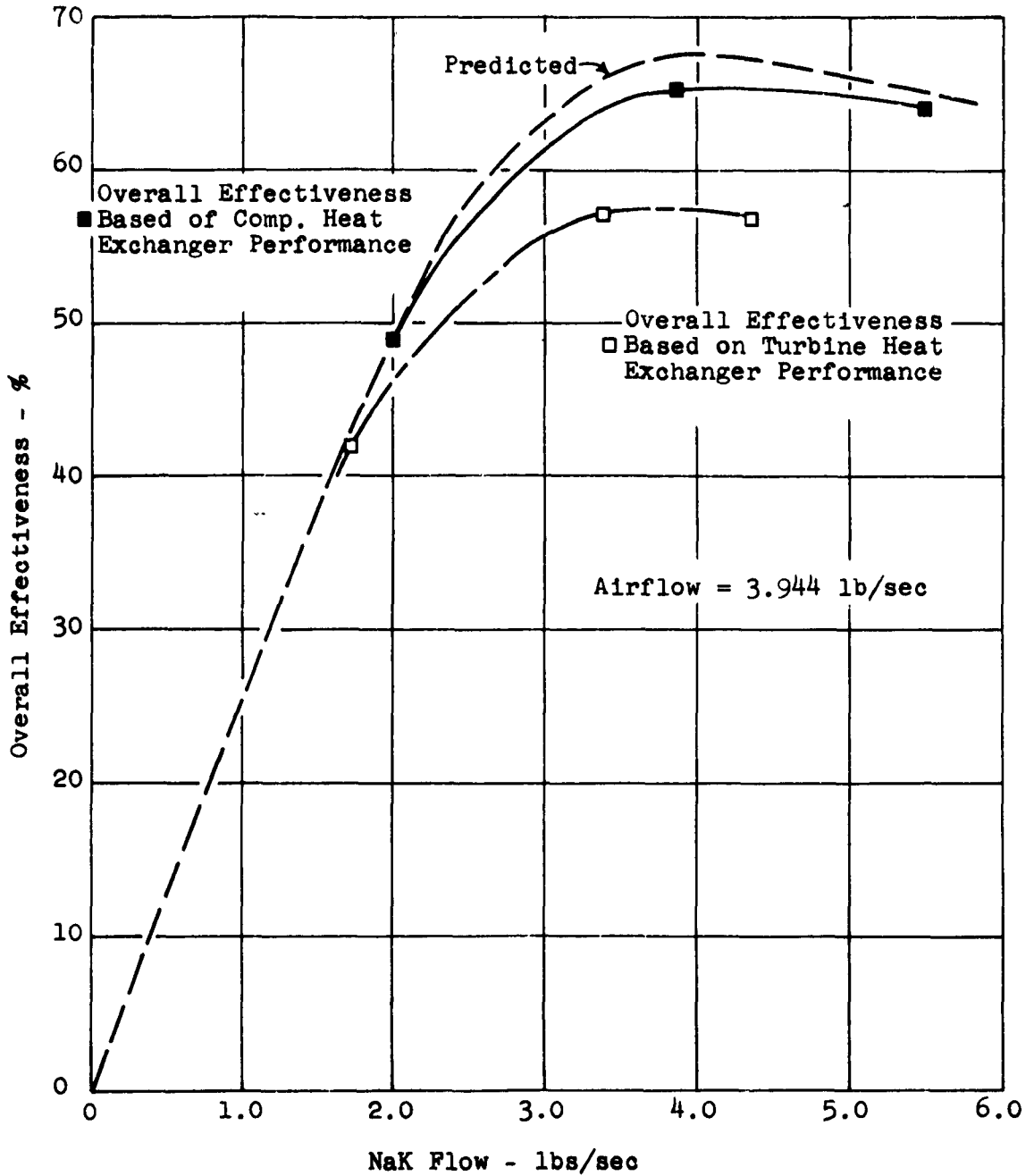
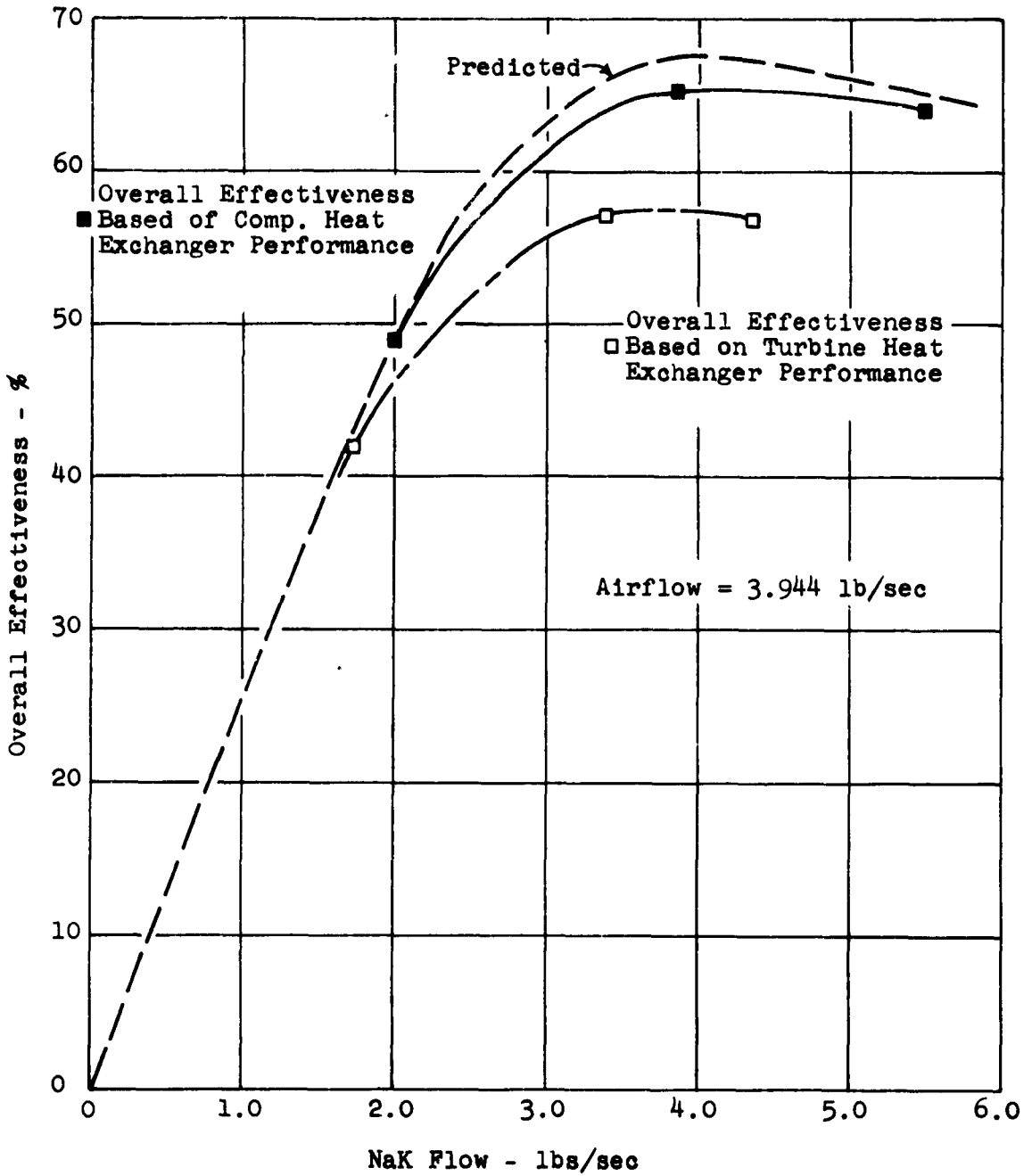


Figure 9.3-3

OVERALL EFFECTIVENESS
vs
CORRECTED NaK FLOW



5783

Figure 9.3-3

OVERALL EFFECTIVENESS
vs
CORRECTED NaK FLOW

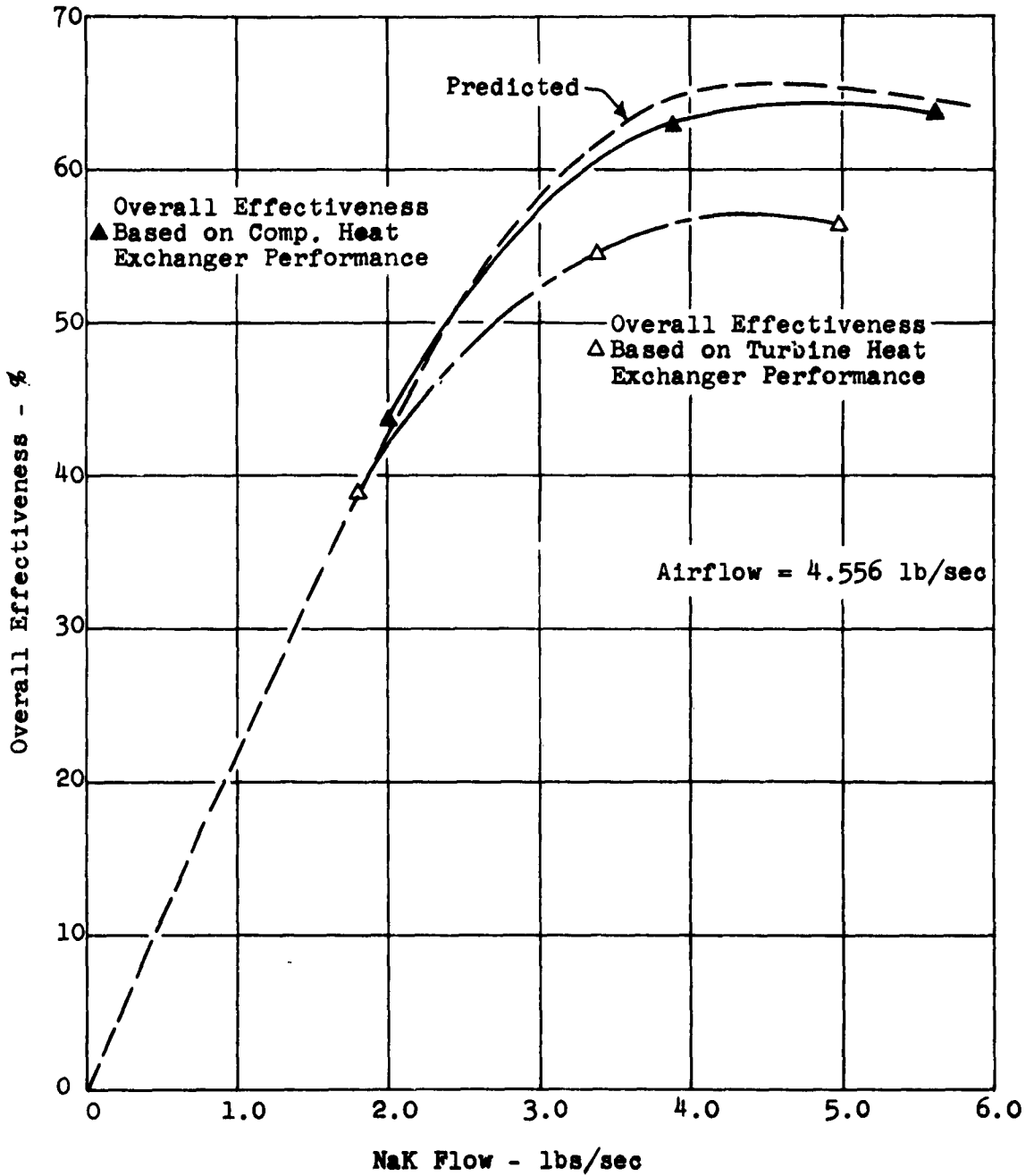


Figure 9.3-4

5784

Inability to hold tolerances in the finned lengths of the serpentine heat transfer elements resulted in excessive exposure of unfinned tubes at the return bends. These areas of low resistance were conducive to bypassing of gas over areas of low heating surface. The amount of bypass is unpredictable because of the random nature of contributing causes. A review of manufacturing techniques indicates that control of the finned lengths can be obtained with proper tooling, and that negative effects from this source can be eliminated in future work.

Pressure drop through the turbine heat exchanger was obtained from root mean square values of readings across the heat exchanger. Measured $\Delta P/P$ is plotted, with predicted values, in Figure 9.3-5 for the parameter $W\sqrt{T}/P$. Pressure drop through the compressor heat exchanger is subject to error, having been obtained as small differences of large pressure readings. The variations in air pressure were of magnitudes approaching the pressure drop through the heat exchanger. A plot of measured $\Delta P/P$ and predicted $\Delta P/P$ versus the flow parameter $W\sqrt{T}/P$ is shown in Figure 9.3-6. The cluster of points is the result of the method of testing in which the throttle valve downstream of the compressor heat exchanger was kept fixed. Since critical pressure ratio across the throttle valve was exceeded, the term $W\sqrt{T}/P$ remained practically constant. The low magnitude of $\Delta P/P$ is attributed to the experimental error and effects of distribution previously discussed.

9.4 Liquid Metal

The liquid metal responded well to all modes of operation and produced no operating problems. However, heat balances between the liquid metal and the gas could not be obtained. The indicated liquid metal heat capacity was consistently lower than the gas side heat capacity. Evaluation of all factors lead to the conclusion that the liquid metal flow exceeded that indicated by the flow-meter and it is believed that an unevaluated error was introduced by the substitution of a larger flow pipe into the meter to reduce line losses. The tight test schedule and the complexity of removing the flow-meter from the system prevented calibrating tests from being made.

Liquid metal flow was controlled by varying the speed of the pump. Liquid metal flow could be increased or decreased at will without changing air flow or fuel flow. The temperature response of the system rapidly followed changes in liquid metal flow.

TURBINE HEAT EXCHANGER
PRESSURE DROP vs FLOW FACTOR

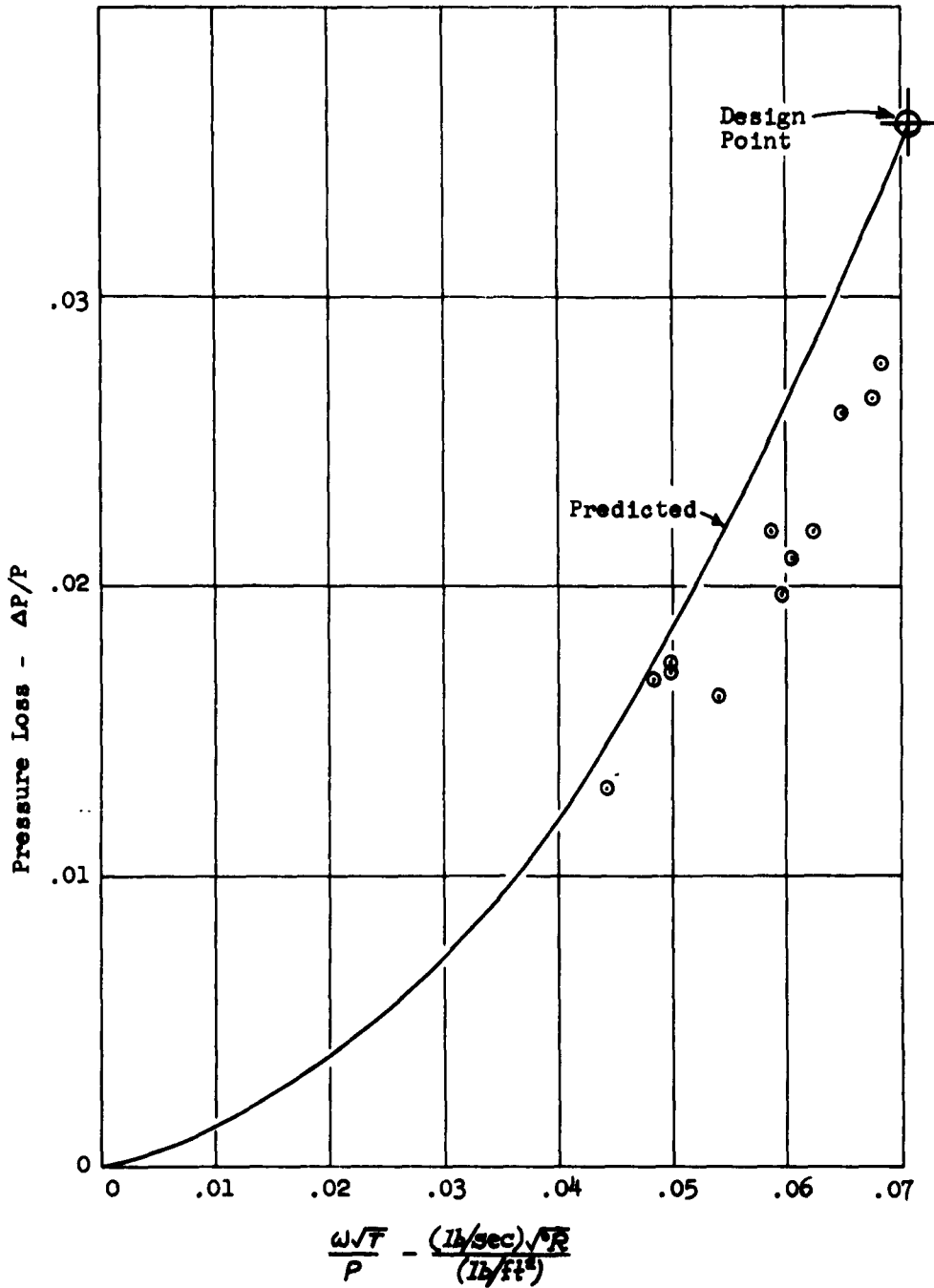


Figure 9.3-5

5785

COMPRESSOR HEAT EXCHANGER
 PRESSURE DROP VS FLOW FACTOR

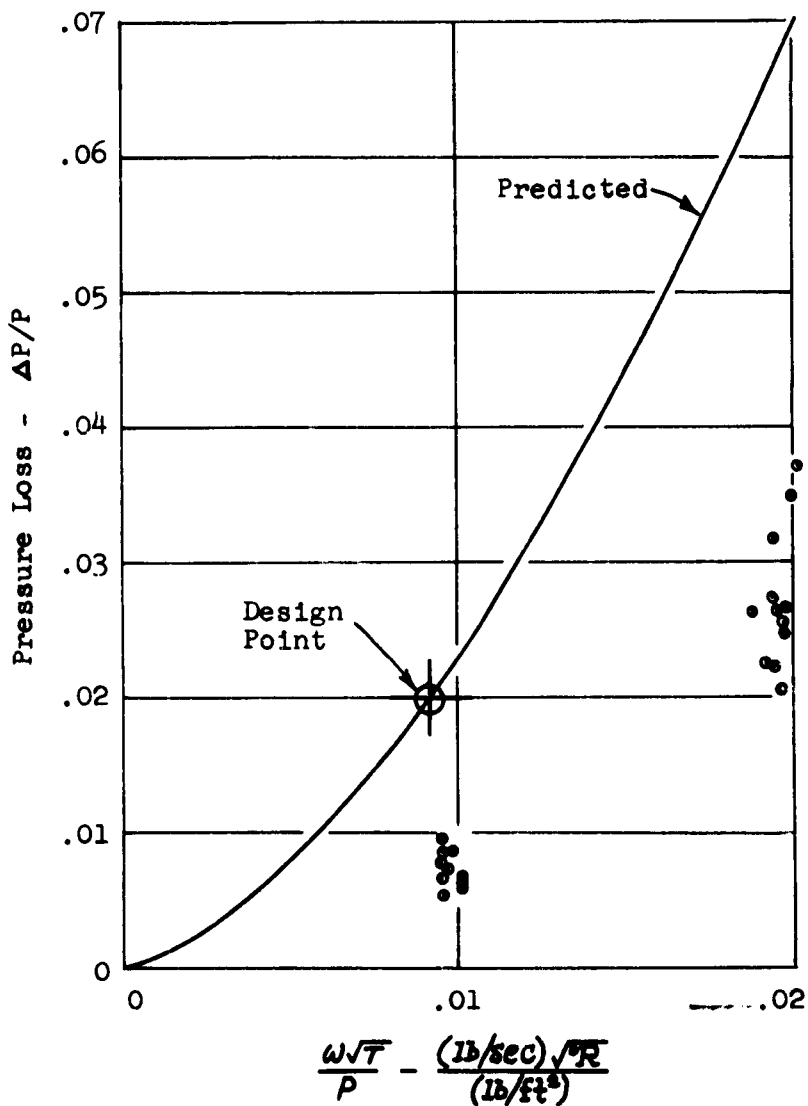


Figure 9.3-6

5787

9.5 Fouling

Inspection of the heat exchangers after 40 hours of varied operation showed no build-up of soot deposits except on the trailing edge of the last row of tubes in the turbine heat exchanger. Upstream faces and those tubes which could be seen in the body of the heat exchanger were free of deposits. It was evident that areas having high gas velocity are unaffected by soot deposits. However, at regions of sudden reduction of velocity, as at the trailing edge of the last row of tubes in the turbine heat exchanger, shallow soot deposits can form (Figure 9.5-1). Faint evidence of this action is seen in the last rows of the compressor heat exchanger.

Figure 9.5-2 shows the downstream face of the compressor heat exchanger reflected in a mirror. The upstream face of this heat exchanger is shown in Figure 9.5-3. The upstream face of the turbine heat exchanger was observed to be in similar condition but was not accessible for photographing.

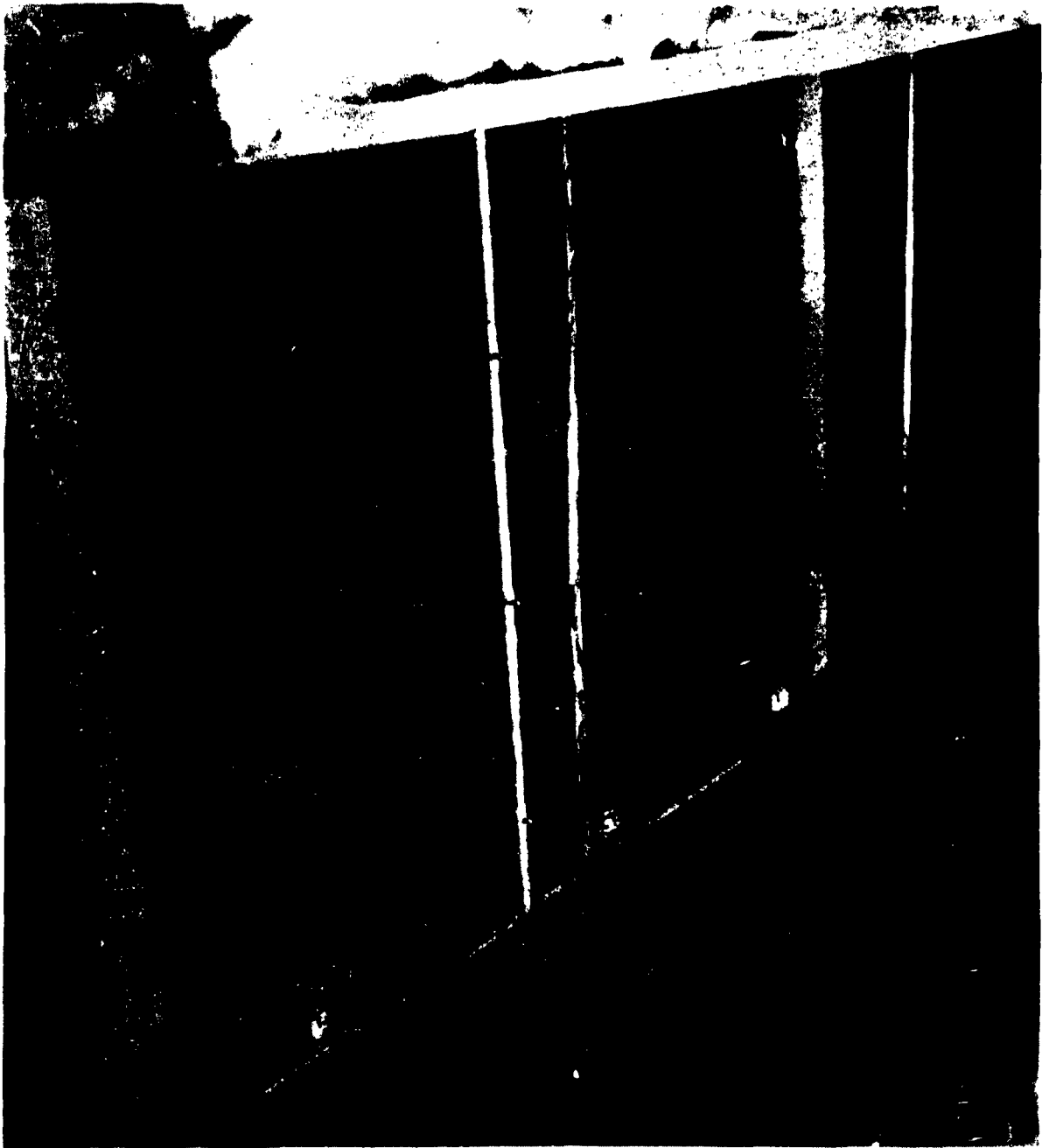
During the 41 hours of continuous operation at cruise conditions continuous - performance curves (Figure 9.5-4) showed little change until after 20 hours of operation, when burner performance started to decline. The exhaust became smokey and fuel flow had to be increased to maintain burner exit temperature. Operation was continued for 21 hours until burner performance became extremely erratic and forced a shutdown. Overall effectiveness deteriorated slowly with time and dropped to approximately 80% of maximum. It was demonstrated from this run that regenerator action can be maintained for prolonged periods with abnormal burner conditions. The slight increase in pressure drop would not be expected to seriously impair performance of an engine.

9.6 Liquid Metal Pump

The demonstration liquid metal pump performance remained substantially constant for each operating speed throughout the full test period. Maximum pump speed could not be obtained towards the end of the test period because of slipping in the special belt-drive. The belt-drive was used as a speed increaser and is not indicative of flight hardware.

Although the liquid metal pump met the requirements of this program further efforts were made to improve the performance of the pump. Internal pin stays extending through the liquid metal flow path in the pump cell caused hydraulic losses within the cell which reduced the useful pressure rise generated in the pump. A subsequent pump cell design, utilizing elliptical walls, eliminated the internal pins. Performance tests by the manufacturer have demonstrated a 50% reduction

TURBINE HEAT EXCHANGER
Downstream Face After 40 Hours Operation



4761

Figure 9.5-1

COMPRESSOR HEAT EXCHANGER
Mirror Image of Downstream Face After 40 Hours
Operation with Preheater



4764

Figure 9.5-2

MPR...OR...AT...HAN...
After 40 Hours Operation with Preheater



Figure 9.5-3

LIQUID METAL REGENERATOR SYSTEM
 PERFORMANCE vs TIME
 Design Point Operation - 1500 Ft. 225KN 35% NRP

- 30 GPM Nak flow
- - - 25 GPM Nak flow
- · - · 20 GPM Nak flow

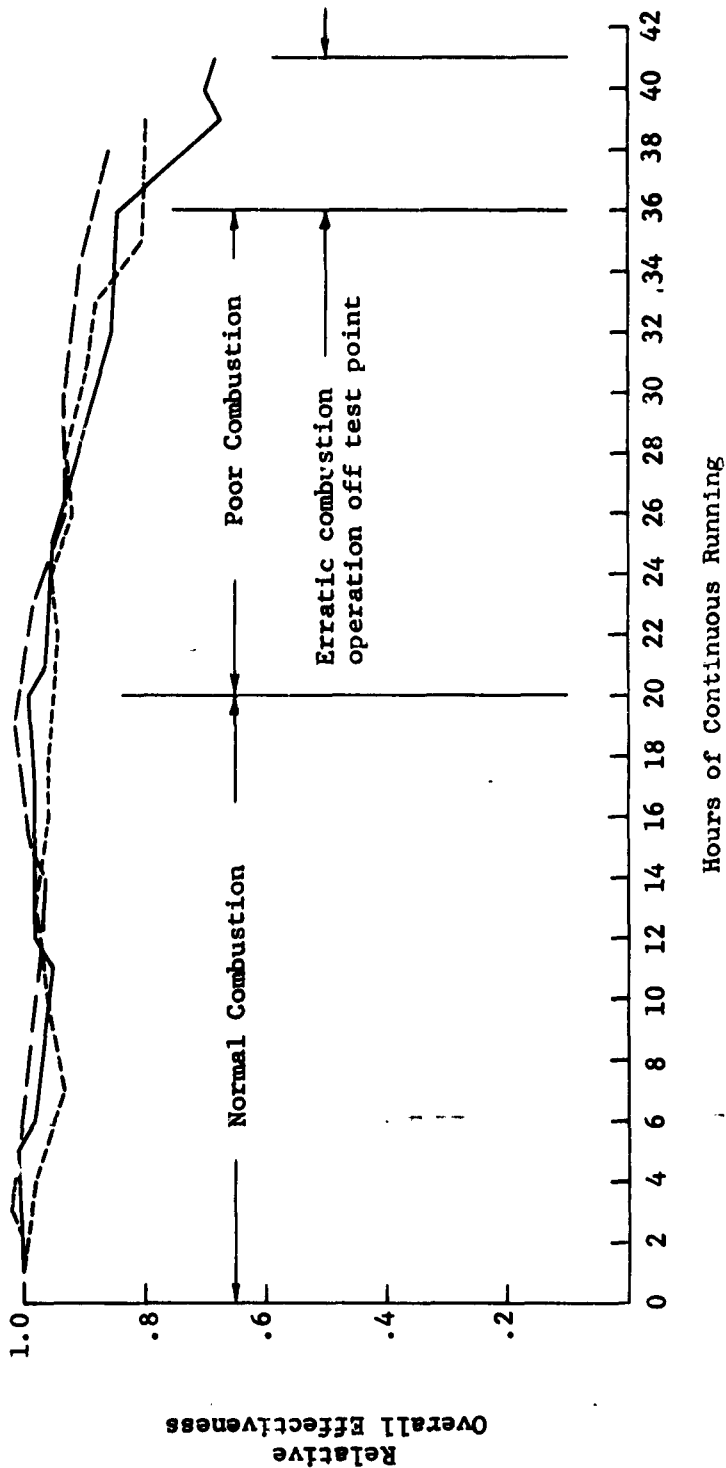


Figure 9.5-4

in internal hydraulic losses. Procurement of this cell was too late to be included in the liquid metal circuit.

The prototype pump successfully demonstrated that the pump cell can be made in independent sectors, with each sector connected to separate liquid metal loops. The pump also demonstrated that a rotor containing permanent magnets can pump liquid metals and requires no external source of electric power. These achievements indicate that a light-weight pump can be developed for aircraft engines.

9.7 Liquid Metal Alloys

A short investigation was conducted to find liquid metal alloys retaining a high percentage of liquid at -65°F . Various compositions of an alloy of cesium and NaK (up to 50% cesium) were investigated. The amount of metal liquid at -65°F is proportional to the amount of cesium and is 98% liquid for 55% cesium. (Table 9.7-1). Tests were conducted in apparatus simulating the major components of a liquid metal regenerator system to determine the cold start behavior of NaK 56 and 10% cesium NaK. The two liquid metal alloys and their respective test apparatus were chilled by means of a cold box to $+50^{\circ}\text{F}$, -15°F , and -65°F prior to placement in the exhaust of the test engine which was then immediately started. Test conditions were more severe than normal start up conditions in that gas flow was unusually high and was concentrated on only a portion of the chilled heat transfer element. Both systems responded favorably at 50°F initial conditions. At -15°F initial conditions, the NaK 56 system had the heat transfer element severely distorted. The 10% cesium NaK system showed a minor distortion which was attributed to the severe aerodynamic loading at the test conditions. At -65°F both systems ruptured in the heat transfer element. These screening tests have shown that the addition of small amounts of cesium to a NaK alloy can make significant improvements in the cold-start behavior of a liquid metal regenerator system under severe starting conditions. The favorable results indicate that further work should be done under more realistic conditions to determine the optimum alloy.

LIQUID-SOLID RATIO AT -65°F

For Various Cesium Additions to Nak 77 (77% potassium)

Weight % Cesium	Weight % Liquid
5	9
10	18
15	27
20	36
25	45.5
30	53
35	62
40	71
45	80
50	89
55	98

Table 9.7-1

9.8 Analytical Methods, References

The design of the heat exchangers and the evaluation of heat exchanger performance followed methods described by Kays and London in "Compact Heat Exchangers" (National Press, Palo Alto, California, 1955). Certain adaptations, described below, were made to include specific heat transfer matrix data, and to establish calculation procedures best suited for designing liquid metal regenerator systems for turbine engines. Definitions of the symbols and units employed are listed in Section 10, which follows.

Experimental data, previously obtained from similar heat transfer matrices, has been reduced to the following friction and heat transfer relationships which are applicable to the present range of design conditions. These relations are, respectively,

$$f = 0.17926 \left(\frac{1}{N_R} \right)^{.205},$$

$$N_{ST} = 0.0156 \left(\frac{1000}{N_R} \right)^{.435}.$$

Selections are made of numbers of tube rows and maximum velocities which satisfy, in combination, the previously specified pressure drops through the heat exchangers. The selected values of number of tube rows and gas velocities are then used in the following equation, to obtain the value of $nv(1.795)$,

$$nv(1.795) = \frac{(\Delta P/P) (D_e)^{1.205} (P) g}{\left(2 \frac{L}{n} \right) (\mu)^{.205} (0.17926) (\rho)}.$$

In the denominator, the factor L/n denotes the distance between center-lines of adjacent tube-rows, measured in the direction of gas flow. The preceding equation is obtained by rearrangement of the equation which relates matrix friction-factor and pressure drop, - that is, from the equation

$$\frac{\Delta P}{P} = \frac{4fL \rho v^2}{D_e (2g) P}.$$

Heat exchanger geometries and values of N_R can now be established by conventional methods. The various heat exchanger geometries can be examined for heat transfer performance. Gas side heat transfer rates are obtained from the Stanton-number (N_{ST}) relationship which is given above for the heat transfer matrix.

Liquid metal side heat transfer rates are obtained by methods described in the "Liquid-Metals Handbook, Sodium-NaK Supplement" (AEC, Department of Navy, 1 July, 1955). The number of transfer units (NTU) relationships are obtained as described in "Compact Heat Exchangers" for the selected heat exchanger geometries, and the corresponding individual effectivenesses are calculated. The individual effectivenesses are combined to provide the value of overall effectiveness in the equation,

$$E_o = \frac{1}{\frac{1}{E_c} + \frac{1}{E_h} - 1}$$

By a reiterative process, the number of tube rows required to provide the required overall effectiveness is determined. The alternative solutions, each satisfying the initial requirements of heat transfer, effectiveness and pressure drop, are compared with respect to weight, face area and practicality of tube-row arrangements. Optimum design is accomplished by choice from the results of this comparison.

A detailed step-by-step description of the design method outlined above has previously been presented by the Curtiss-Wright Corporation in TREC Technical Report 61-46, dated April, 1961. This report covers an analysis made in connection with a feasibility program, prior to the work of the present program.

The detailed considerations of geometry and metals upon which design of the heat exchangers of this program was based can be found in Wright Aeronautical Serial Report CTR.00-272, entitled, "Advanced Heat Transfer Elements for Liquid Metal Regenerator Systems".

10. SYMBOLS

A	Area - Heat Transfer Surface	ft ²
A _{fc}	Face Area - Compressor Heat Exchanger	ft ²
A _{fh}	Face Area - Turbine Heat Exchanger	ft ²
C	Flow Stream Capacity Rate (W C _p)	BTU/hr-°F
C _p	Specific Heat at Constant Pressure	BTU/lb-°F
D _e	Equivalent Hydraulic Diameter	ft
E _c	Effectiveness - Compressor Heat Exchanger	-
E _h	Effectiveness - Turbine Heat Exchanger	-
E _o	Overall Regenerator Effectiveness	-
f	Fanning Friction Factor	-
G	Mass Velocity	lb/hr-ft ²
g	Acceleration of Gravity	ft/sec ²
h	Heat Transfer Film Coefficient	BTU/hr-ft ² -°F
L	Core Length	ft
N _c	Tube Rows - Compressor Heat Exchanger	-
N _h	Tube Rows - Turbine Heat Exchanger	-
N _R	Reynolds Number (D _e G/μ)	-
N _{ST}	Stanton Number (h/G C _p)	-
NTU	Number of Heat Transfer Units (AU/C _{min})	-
n	Number of Tube Rows	-
P	Total Pressure	lbs/ft ²
T	Absolute Temperature, Degrees Rankine	°R
TET	Turbine Entry Temperature	°R

U	Overall Heat Transfer Coefficient	BTU/hr-ft ² -°F
v	Velocity	ft/sec
W _c	Weight Flow - Compressor Heat Exchanger	lb/sec
W _h	Weight Flow - Turbine Heat Exchanger	lb/sec
(ΔP/P) _c	Pressure Drop - Compressor Heat Exchanger	-
(ΔP/P) _h	Pressure Drop - Turbine Heat Exchanger	-
(ΔP/P) _o	Pressure Drop - Total of Heat Exchangers	-
μ	Viscosity	lb/sec-ft
ρ	Density	lb/ft ³